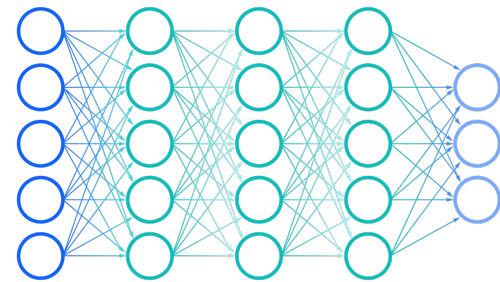
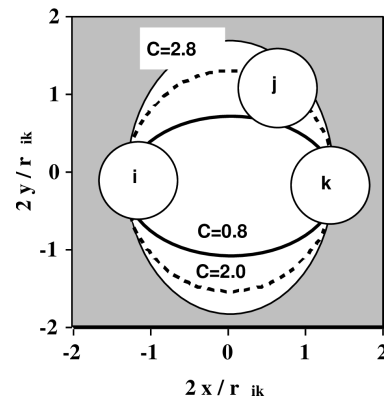
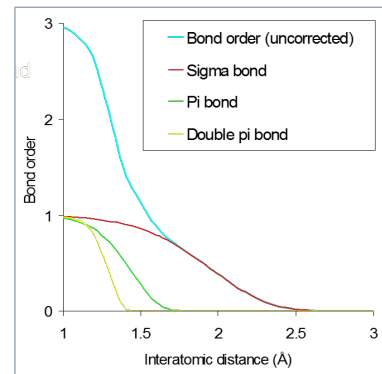
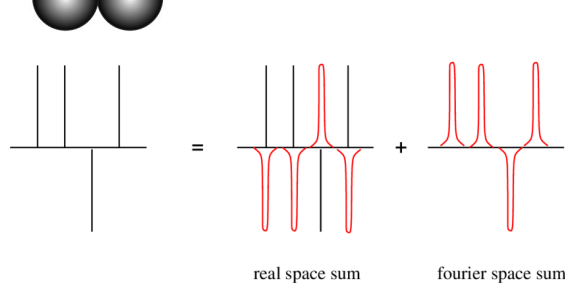
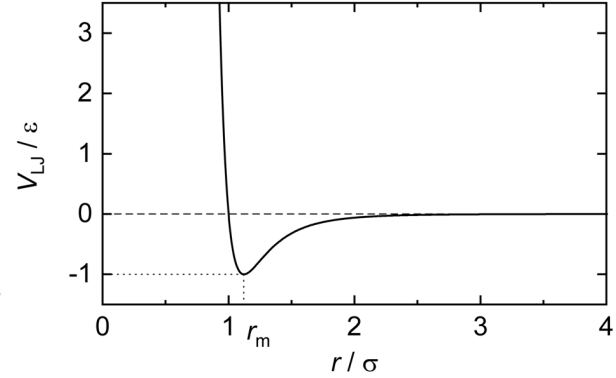
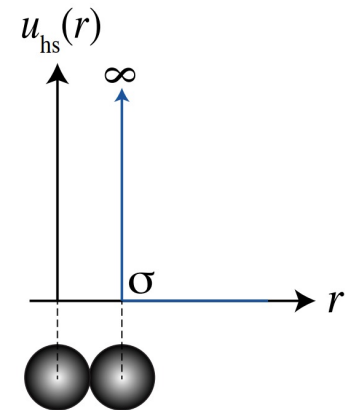


The Past, Present, and Future of Forcefield Technologies

September 19–21, 2023



Materials Design Webinar Series

- Each session runs several times to accommodate schedules
 - Share the webinar series with your colleagues!
 - Registration details <http://www.materialsdesign.com/webinars>
- We will be recording this webinar
 - Watch any of our earlier webinars anytime
 - We will post upcoming webinars on the webinar page
- Vote for the next webinar topic!
 - Take a 2 minutes brief survey at the end of the webinar!

Please Ask Questions!

The screenshot shows the 'GoToWebinar Control Panel' with several sections:

- Audio:** Includes a microphone icon, 'Computer audio' (selected) and 'Phone call' options, a 'MUTED' status, and dropdown menus for 'Built-in Microphone' and 'Built-in Output'. A volume bar is also present.
- Talking:** Shows 'Katherine Hollingsworth' as the current speaker.
- Questions:** A list of questions and answers. One question is highlighted: 'Q: Can you calculate the gelation point of a polymer?' with the answer: 'A: Yes we can! David will address this on an upcoming slide soon.'
- Input Field:** A text box containing 'What forcefields are supported by MedeA?' and a 'Send' button with a paper plane icon.

Annotations with green arrows point to specific features:

- 'full screen' points to the top-right icon in the sidebar.
- 'during discussion: raise hand to speak' points to the hand icon in the sidebar.
- 'any time during webinar: type your question here and then press Send' points to the text input field and the Send button.

Use the raise hand icon to bring attention to your question



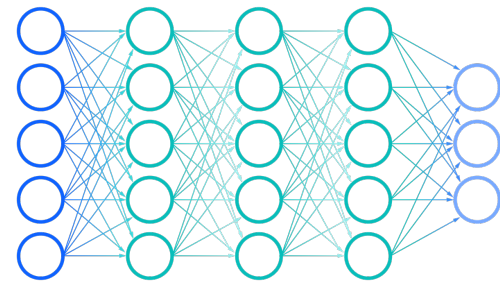
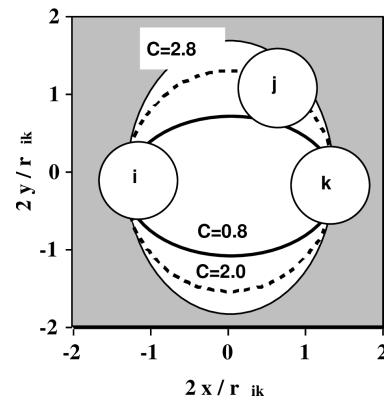
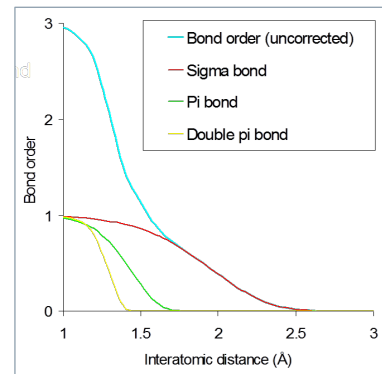
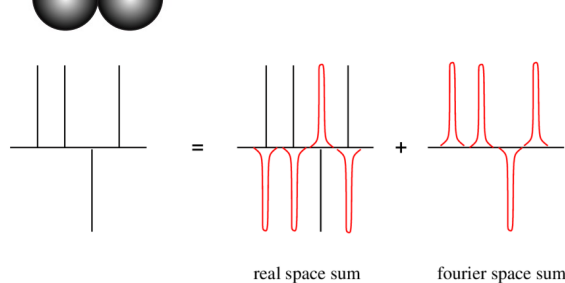
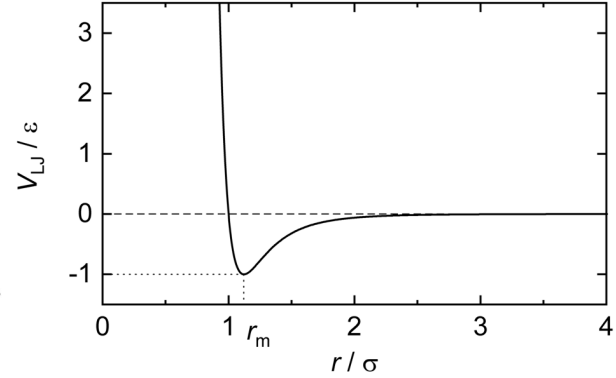
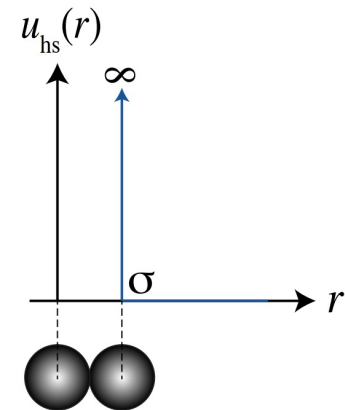
Webinar Speakers

Katherine Hollingsworth

Presenter: Dr. Garrett Tow

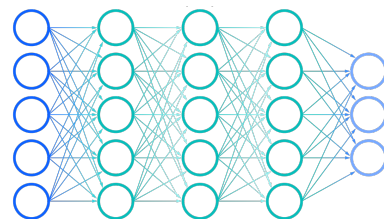
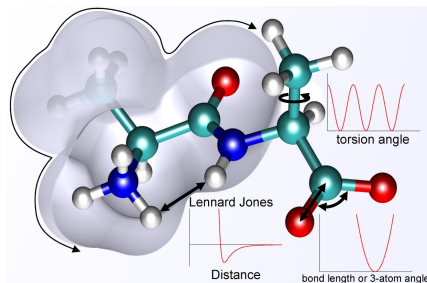
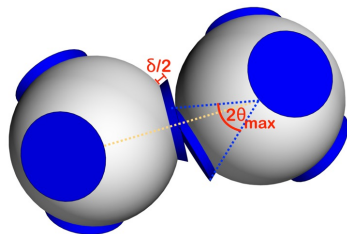
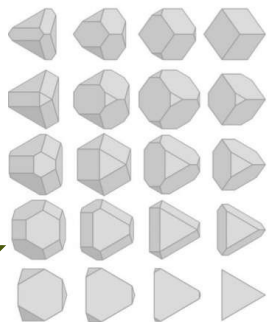
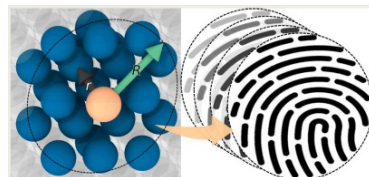
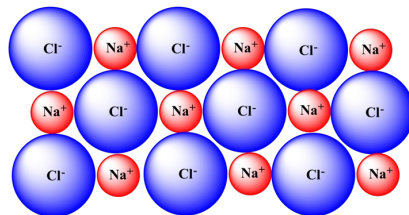
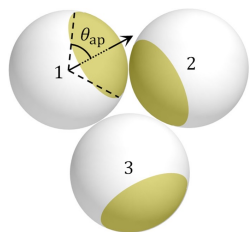
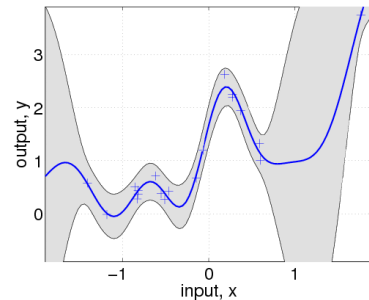
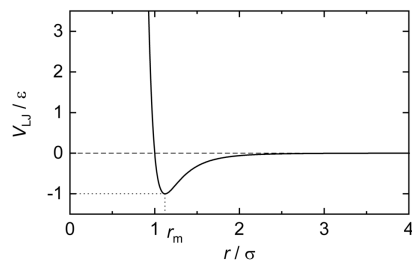
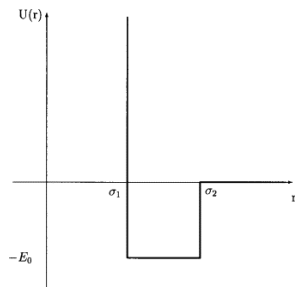
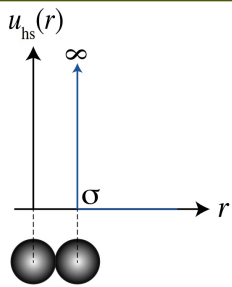
The Past, Present, and Future of Forcefield Technologies

September 19–21, 2023



Versatility of Functional Form

Embellishments and Complexity



Forcefield = Hamiltonian

The Hamiltonian is an operator describing the total energy of a system.

Typical forcefield parameters:

- Repulsion–dispersion (ϵ, σ)
- Energy coefficients for bonded terms (k_b, k_θ, k_ϕ)
- Nominal bond lengths, bond angles, and dihedrals (b_0, θ_0, ϕ_0)
- Partial point charges (q_i)
- Particle masses (m_i)
- Pairwise cutoff distance (r_{cut})
- Analytical tail corrections

Time-Dependent Schrödinger Equation

$$H |\psi(t)\rangle = i\hbar \frac{\partial}{\partial t} |\psi(t)\rangle$$

$$H = T + U$$

$$T = \frac{1}{2} \sum_{atoms} m v^2$$

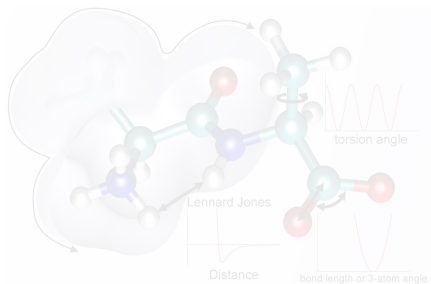
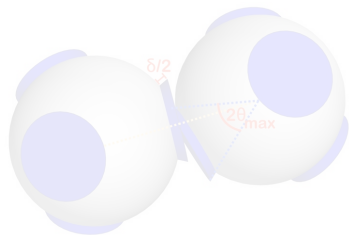
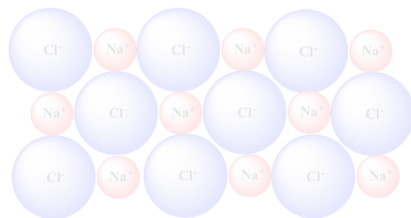
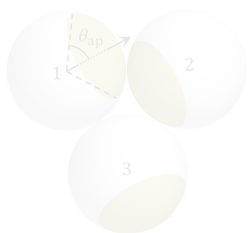
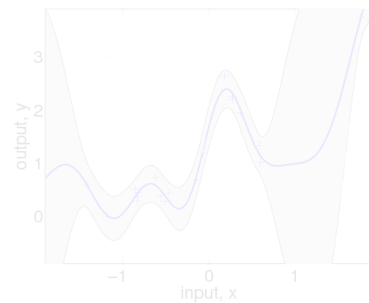
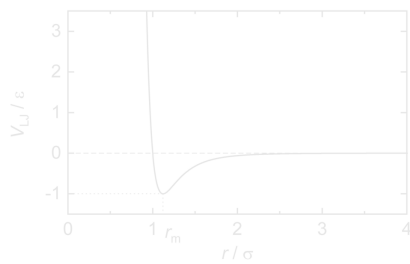
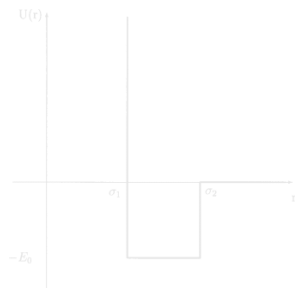
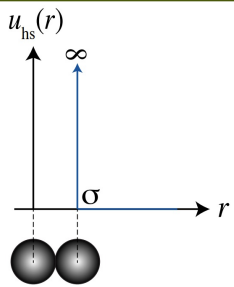
$$U = \frac{1}{2} \sum_{bonds} k_b (b - b_0)^2 + \frac{1}{2} \sum_{angles} k_\theta (\theta - \theta_0)^2 + \frac{1}{2} \sum_{improper} k_\phi (\phi - \phi_0)^2 +$$

$$\frac{1}{2} \sum_{torsions} k_\phi [1 + \cos(n\phi + \delta)] + \sum_{atom\ pairs\ ij} \left[\frac{q_i q_j}{R_{ij}} + \frac{A_{ij}}{R_{ij}^{12}} - \frac{B_{ij}}{R_{ij}^6} \right]$$

Example forcefield (Hamiltonian) of a molecular model.

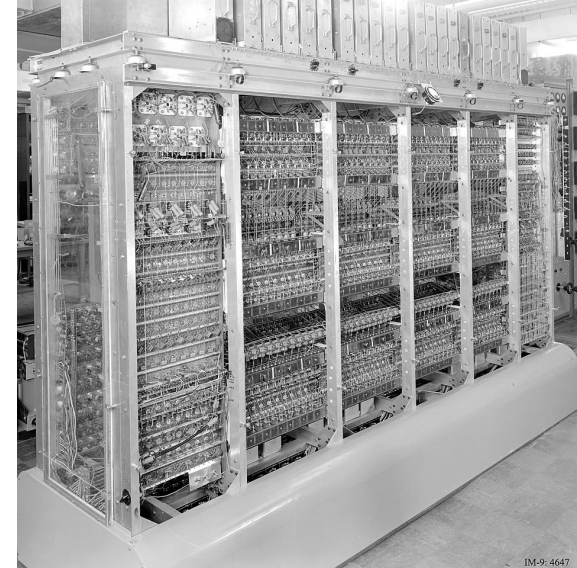
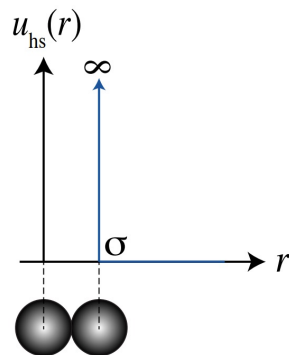
Versatility of Functional Form

Embellishments and Complexity



In the Beginning – Hard Spheres

$$V(\mathbf{r}_1, \mathbf{r}_2) = \begin{cases} 0 & \text{if } |\mathbf{r}_1 - \mathbf{r}_2| \geq \sigma \\ \infty & \text{if } |\mathbf{r}_1 - \mathbf{r}_2| < \sigma \end{cases}$$



THE JOURNAL OF CHEMICAL PHYSICS

VOLUME 21, NUMBER 6

JUNE, 1953

Equation of State Calculations by Fast Computing Machines

NICHOLAS METROPOLIS, ARIANNA W. ROSENBLUTH, MARSHALL N. ROSENBLUTH, AND AUGUSTA H. TELLER,
Los Alamos Scientific Laboratory, Los Alamos, New Mexico

AND

EDWARD TELLER,* *Department of Physics, University of Chicago, Chicago, Illinois*

(Received March 6, 1953)

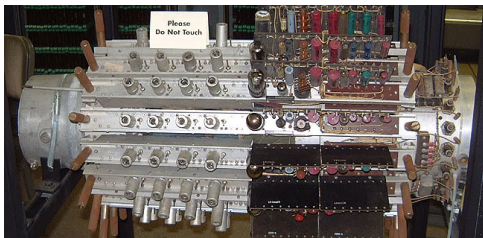
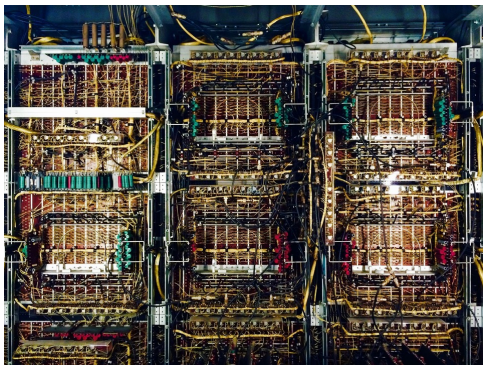
A general method, suitable for fast computing machines, for investigating such properties as equations of state for substances consisting of interacting individual molecules is described. The method consists of a modified Monte Carlo integration over configuration space. Results for the two-dimensional rigid-sphere system have been obtained on the Los Alamos MANIAC and are presented here. These results are compared to the free volume equation of state and to a four-term virial coefficient expansion.

MANIAC

- 224 particles
- 5 hours to determine P for given V
- Metropolis Monte Carlo

Hard Sphere Molecular Dynamics

UNIVAC I



Mercury delay-line memory of UNIVAC

- 32 particles
- 10• 300 collisions per hour

IBM-704

N	Collisions / hour
32	7000
108	2000
256	1000
500	500

Collisions are determined algebraically

Phase Transition for a Hard Sphere System

B. J. ALDER AND T. E. WAINWRIGHT

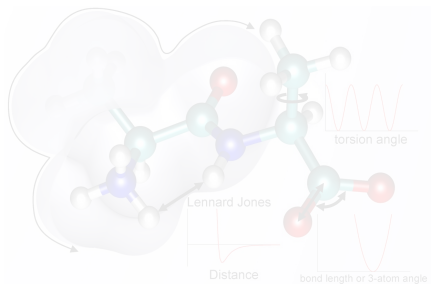
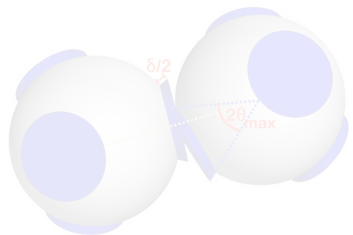
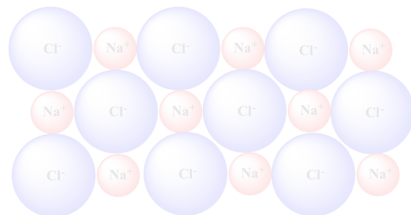
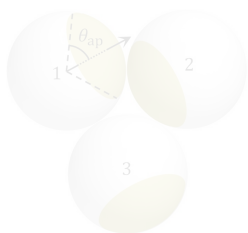
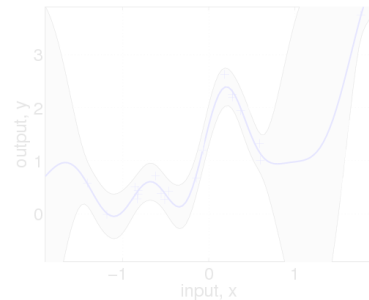
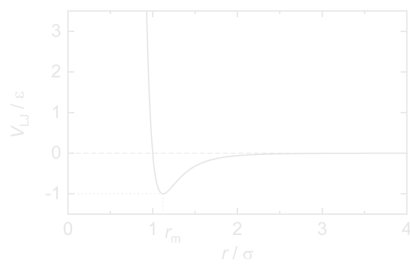
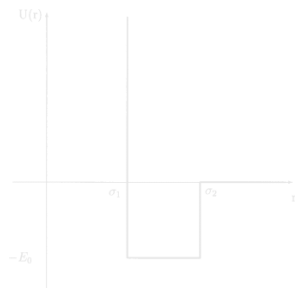
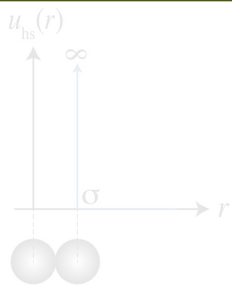
University of California Radiation Laboratory, Livermore, California

(Received August 12, 1957)



Versatility of Functional Form

Embellishments and Complexity



Square-Well Potentials

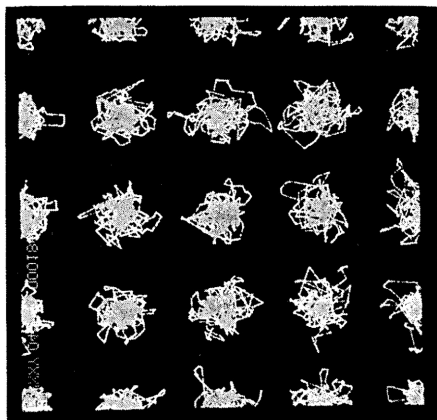


FIG. 2. The traces of 32 hard sphere particles in the periodic boundary conditions in the solid phase for about 3000 collisions.

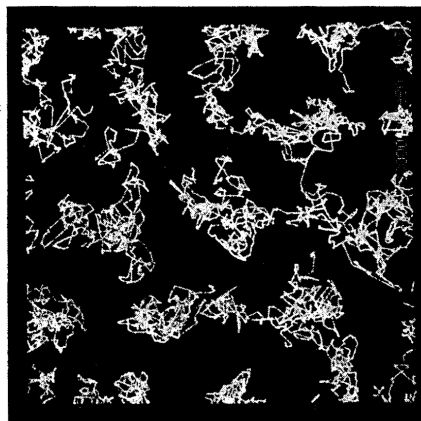
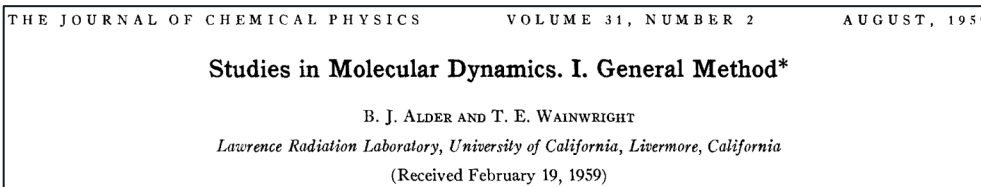
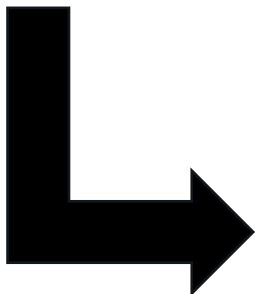
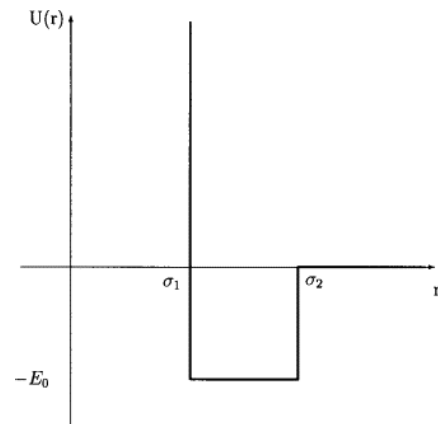


FIG. 3. The traces of the same system as in Fig. 2 after it has transformed to the fluid phase also for 3000 collisions.



(1) core collision

$$\Delta \mathbf{v}_i = -\Delta \mathbf{v}_j = \frac{-\mathbf{r}_{ij} b_{ij}}{\sigma_1^2}$$

(2) attractive collision

(a) $C_{ij}^{(2)} > 0 \ddagger$

“Capture”

$$\Delta \mathbf{v}_i = -\Delta \mathbf{v}_j = \frac{-\mathbf{r}_{ij}}{2\sigma_2^2} \left[\left(\frac{4\sigma_2^2 V_0}{m} + b_{ij}^2 \right)^{\frac{1}{2}} + b_{ij} \right]$$

(b) $C_{ij}^{(2)} < 0 \ddagger$

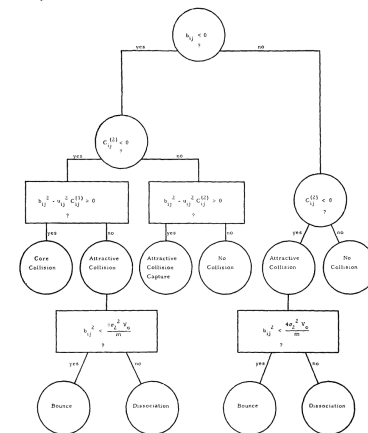
(i) $b_{ij}^2 > \frac{4\sigma_2^2 V_0}{m}$

“Dissociation”

$$\Delta \mathbf{v}_i = -\Delta \mathbf{v}_j = -\frac{\mathbf{r}_{ij}}{2\sigma_2^2} \left[-\left(\frac{-4\sigma_2^2 V_0}{m} + b_{ij}^2 \right)^{\frac{1}{2}} + b_{ij} \right]$$

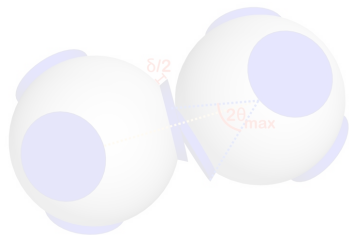
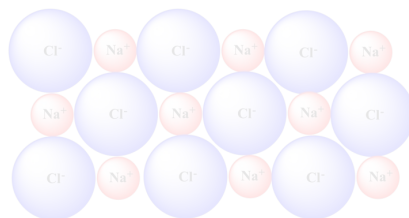
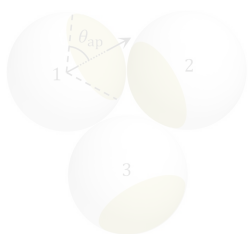
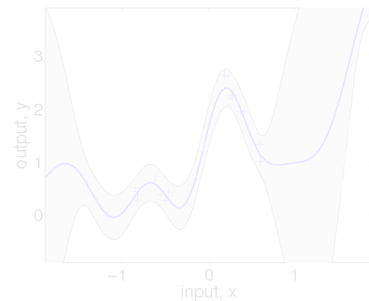
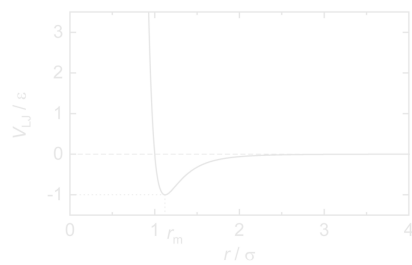
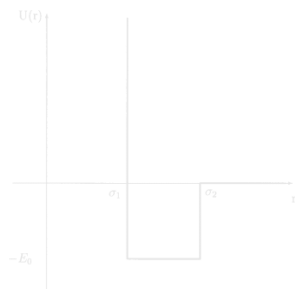
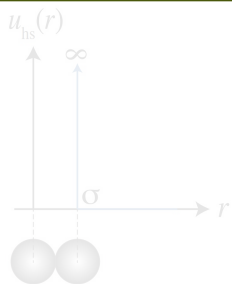
(ii) $b_{ij}^2 < \frac{4\sigma_2^2 V_0}{m}$

“Bounce”



Versatility of Functional Form

Embellishments and Complexity



Pairwise Continuous Potentials

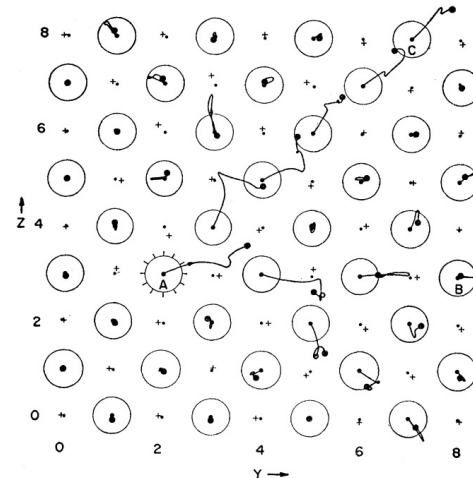
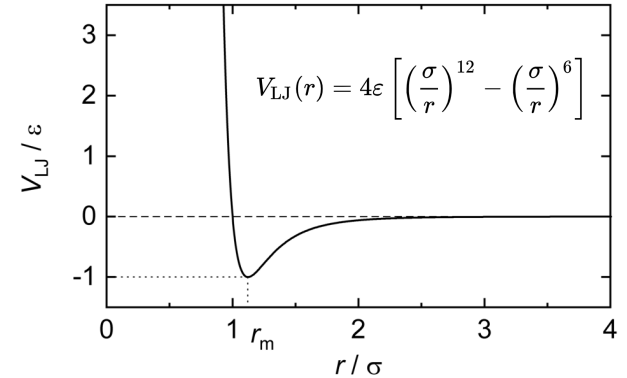
- Lennard-Jones Potential
 - J. E. Lennard-Jones; Cohesion. *Proc. Phys. Soc.* **1931**, 42, 461.
- Lennard-Jones Particle Simulations
 - M. N. Rosenbluth, A. W. Rosenbluth; Further Results on Monte Carlo Equations of State. *J. Chem. Phys.* **1954**, 22, 881–884
 - W. W. Wood, F. R. Parker; Monte Carlo Equation of State of Molecules Interacting with the Lennard-Jones Potential. I. A Supercritical Isotherm at about Twice the Critical Temperature. *J. Chem. Phys.* **1957**, 27, 720–733.
- Simulations of “Real” Materials

$$\varphi = Be^{-\beta r}$$

- Born-Mayer Repulsive Potential for Crystalline Copper
 - J. B. Gibson, A. N. Goland, M. Milgram, G. H. Vineyard; Dynamics of Radiation Damage. *Phys. Rev.*, **1960**, 120, 1229–1253.
- Lennard-Jones Potential for Liquid Argon
 - A. Rahman; Correlations in the Motion of Atoms in Liquid Argon. *Phys. Rev.* **1964**, 136, A405–A411.

$$V_{LJ}(r) = 4\epsilon \left[\left(\frac{\sigma}{r} \right)^{12} - \left(\frac{\sigma}{r} \right)^6 \right]$$

Lennard-Jones Potential



Electrostatics

P. P. Ewald; Die Berechnung optischer und elektrostatischer Gitterpotentiale. *Ann. Phys.* **1921**, 369, 253–287.

A. A. Barker; Monte Carlo Calculations of the Radial Distribution Functions for a Proton–Electron Plasma. *Aust. J. Phys.* **1965**, 18, 119–113

S. G. Brush, H. L. Sahlín, E. Teller; Monte Carlo Study of a One-Component Plasma. I. *J. Chem. Phys.* **1966**, 45, 2102–2118.

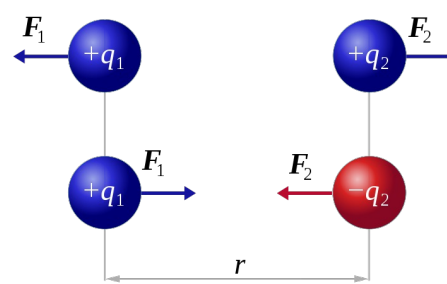
The Enemy: $O(N^2)$

Truncation Methods $O(N)$

- Wolf Summation (discontinuous forces)
- Shifted Force Wolf Summation (poorer energy)
- Modified Shifted Force Wolf Summation
 - *J. Chem. Theory Comput.* **2019**, 15, 572–583.

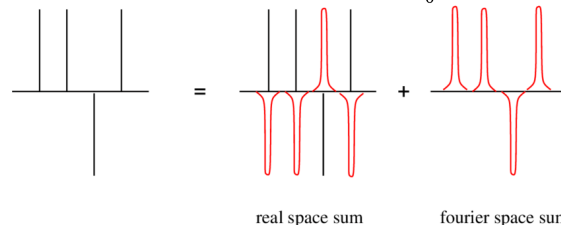
Long-Range Solvers $O(N) - O(N \log(N))$

- Particle–Particle Particle–Mesh (PPPM)
- Particle–Mesh Ewald (PME)
- Fast Fourier Poisson Method (FFP)
- Fast Multipole Algorithm (FMA)
- Reduced Cell Multipole Method (RCMM)
- Macroscopic Multipole Method (MMM)
- PPPM/Multipole Expansion (PPPM/MPE)



$$|F_1| = |F_2| = k_e \frac{|q_1 \times q_2|}{r^2}$$

$$k_e = \frac{1}{4\pi\epsilon_0}$$



Paul Peter Ewald in 1934

Born January 23, 1888
Berlin, Germany

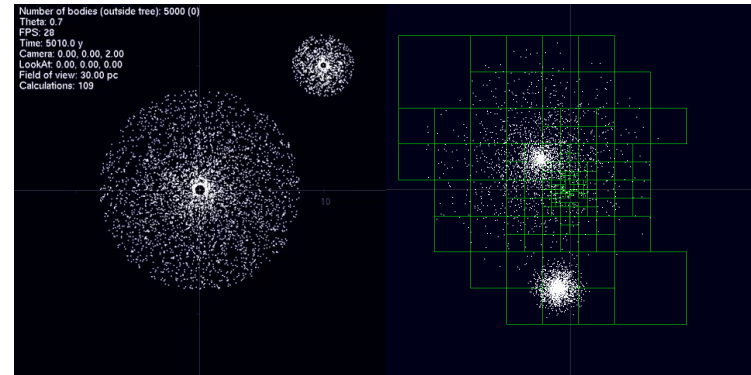
Died August 23, 1985
(aged 97)
Ithaca, New York

n-Body Simulations

$$F = G \frac{m_1 m_2}{r^2}$$

Barnes–Hut Treecode

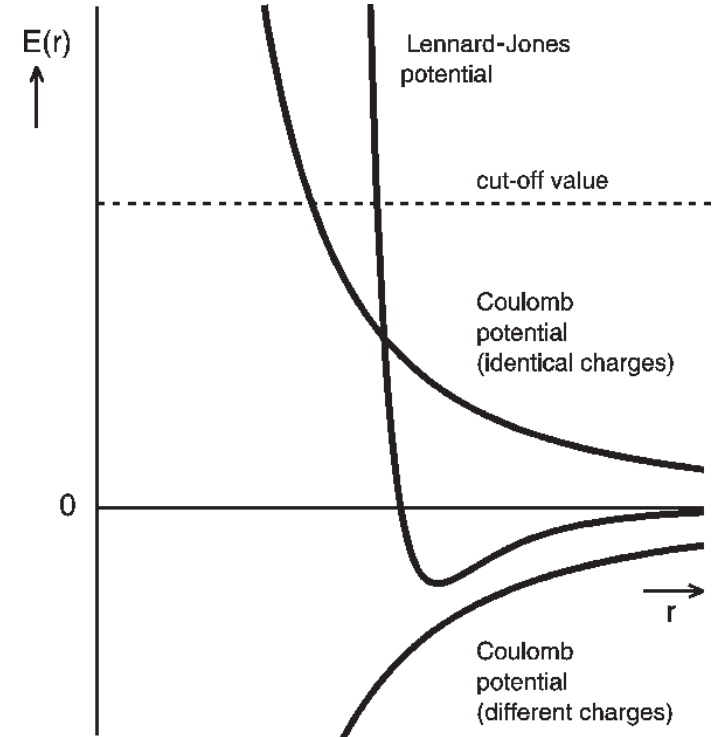
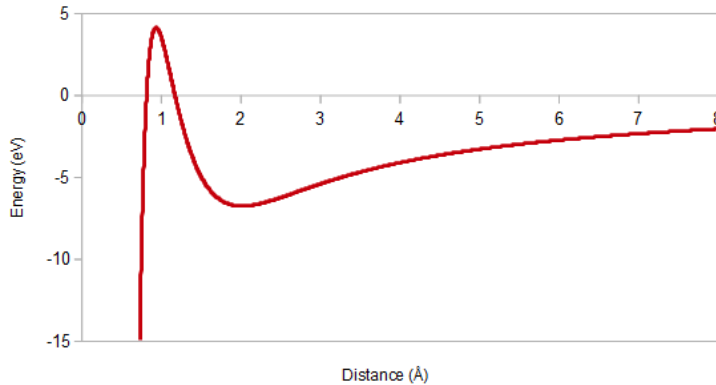
Number of bodies (outside tree): 5000 (0)
Theta: 0.7
FPS: 29
Time: 59.10 0 y
Camera: 0.00, 0.00, 2.00
LookAt: 0.00, 0.00, 0.00
Field of view: 30.00 pc
Calculations: 193



Using Repulsion to Avoid Coulombic Catastrophe

Buckingham Potential

$$U_{BC}(r_{ij}) = A_{ij} e^{-\frac{r_{ij}}{\rho_{ij}}} - \frac{C_{ij}}{r_{ij}^6} + \frac{q_i q_j}{4\pi\epsilon_0 r_{ij}}$$



Responsive Electrostatics

Methods

- Charge Equilibration
- Core–Shell
- Drude Oscillator
- Induced Dipole

Implementations

- Self-Consistent Equilibration
 - Matrix Inversion
 - Iterative Procedures
- Extended Lagrangian

Damping

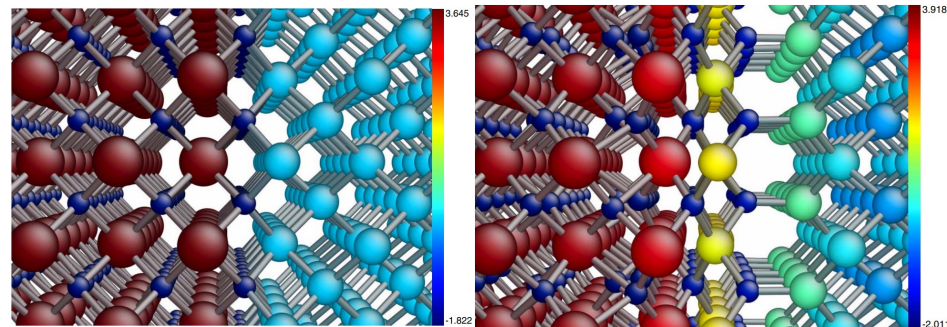
- Thole Damping
- Shielded Coulomb Potential

T.-R. Shan, B. D. Devine, T. W. Kemper, S. B. Sinnott, S. R. Phillpot; Charge-optimized many-body potential for the hafnium/hafnium oxide system. *Phys. Rev. B*, **2010**, *81*, 125328.

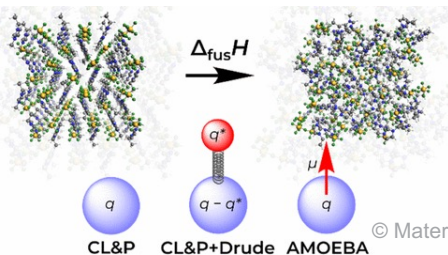
“At a certain level of sophistication it is reasonable to ask whether the models have the physical meaning which is implied or whether we have merely produced convenient parameterisations.” ~Sangster **1973**

M. J. L. Sangster; Interionic Potentials and Force Constant Models for Rocksalt Structure Crystals. *J. Phys. Chem. Solids*, **1973**, *34* 355–363.

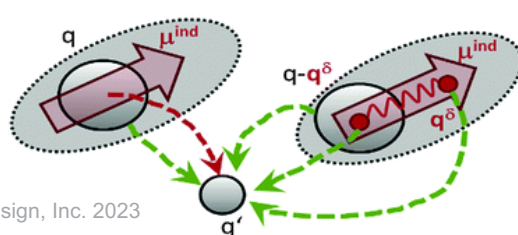
G. Jacucci, I. R. McDonald, K. Singer; Introduction of the shell model of ionic polarizability into molecular dynamics calculations. *Phys. Lett. A*, **1974**, *50*, 141–143.



M. Klajmon, C. Červinka; Does Explicit Polarizability Improve Simulations of Phase Behavior of Ionic Liquids? *J. Chem. Theory Comput.* **2021**, *17*, 6225–6239.



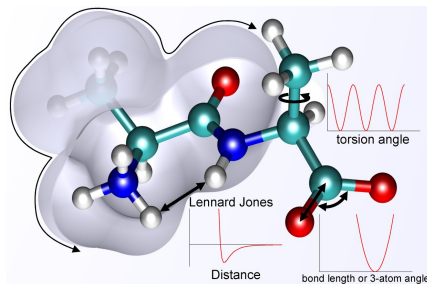
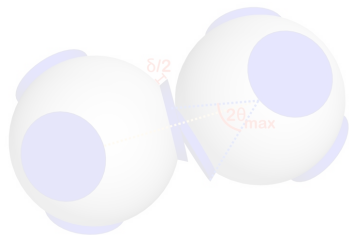
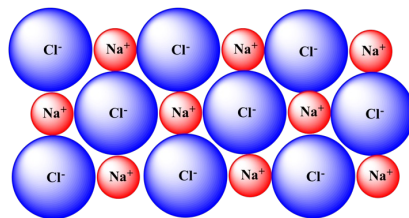
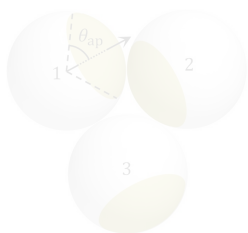
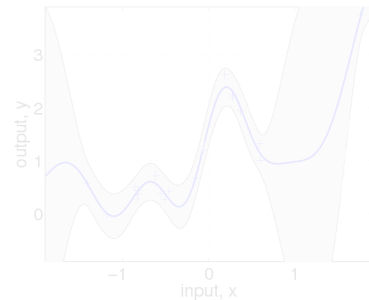
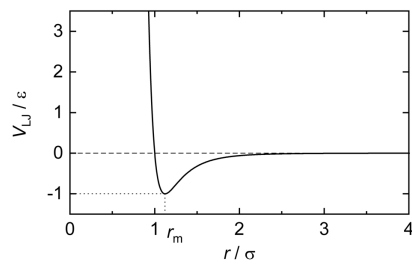
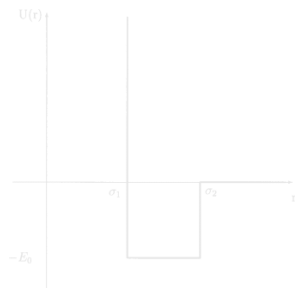
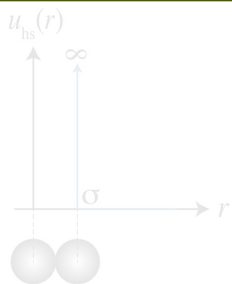
(a) Point-induced dipoles (b) Drude oscillators



M. Schmollngruber, V. Lesch, C. Schröder, A. Heuerb, O. Steinhauser; Comparing Induced Point-Dipoles and Drude Oscillators. *Phys. Chem. Chem. Phys.*, **2015**, *17*, 14297–14306.

Versatility of Functional Form

Embellishments and Complexity



Many-Body Potentials – EAM and MEAM

$$E_i = F_\alpha \left(\sum_{j \neq i} \rho_\beta(r_{ij}) \right) + \frac{1}{2} \sum_{j \neq i} \Phi_{\alpha\beta}(r_{ij})$$

↑ Embedding Energy
↑ Atomic Electron Density
↑ Pair Potential

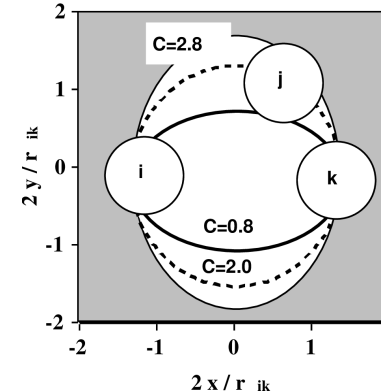
- Embedded-Atom Method (EAM)
 - Considers local coordination effects in addition to pair potential expression.
- Modified EAM (MEAM)
 - Accounts for angular dependence on electron density.
- Multistate MEAM (MS-MEAM)
 - Treats local defects or large strains by reference paths used to determine screening functions.

M. S. Daw, M. I. Baskes; Semiempirical, Quantum Mechanical Calculation of Hydrogen Embrittlement in Metals. *Phys. Rev. Lett.*, **1983**, 50, 1285–1288.

M. S. Daw, M. I. Baskes; Embedded-Atom Method: Derivation and Application to Impurities, Surfaces, and Other Defects in Metals. *Phys. Rev. B*, **1984**, 29, 6443–6453.

M. I. Baskes; Modified Embedded-Atom Potentials for Cubic Materials and Impurities. *Phys. Rev. B*, **1992**, 46, 2727–2742.

M. I. Baskes, S. G. Srinivasan, S. M. Valone, and R. G. Hoagland; Multistate Modified Embedded Atom Method. *Phys. Rev. B*, **2007**, 75, 094113.



M. I. Baskes; Determination of Modified Embedded Atom Method Parameters for Nickel. *Phys. Rev. B*, **1997**, 50, 152–158.

Many Many-Body Potentials

Goal:
Sensitivity to the local
coordination environment

Tersoff

$$E = \frac{1}{2} \sum_i \sum_{j \neq i} V_{ij}$$

$$V_{ij} = f_C(r_{ij} + \delta) [f_R(r_{ij} + \delta) + b_{ij} f_A(r_{ij} + \delta)]$$

$$f_C(r) = \begin{cases} 1 & r < R - D \\ \frac{1}{2} - \frac{1}{2} \sin\left(\frac{\pi}{2} \frac{r-R}{D}\right) & R - D < r < R + D \\ 0 & r > R + D \end{cases}$$

$$f_R(r) = A \exp(-\lambda_1 r)$$

$$f_A(r) = -B \exp(-\lambda_2 r)$$

$$b_{ij} = (1 + \beta^n \zeta_{ij}^n)^{-\frac{1}{2n}}$$

$$\zeta_{ij} = \sum_{k \neq i, j} f_C(r_{ik} + \delta) g[\theta_{ijk}(r_{ij}, r_{ik})] \exp[\lambda_3^m (r_{ij} - r_{ik})^m]$$

$$g(\theta) = \gamma_{ijk} \left(1 + \frac{c^2}{d^2} - \frac{c^2}{[d^2 + (\cos \theta - \cos \theta_0)^2]} \right)$$

J. Tersoff; New Empirical Approach for the Structure and Energy of Covalent Systems. *Phys. Rev. B*, **1988**, *37*, 6991–7000.

Stillinger–Weber

$$E = \sum_i \sum_{j > i} \phi_2(r_{ij}) + \sum_i \sum_{j \neq i} \sum_{k > j} \phi_3(r_{ij}, r_{ik}, \theta_{ijk})$$

$$\phi_2(r_{ij}) = A_{ij} \epsilon_{ij} \left[B_{ij} \left(\frac{\sigma_{ij}}{r_{ij}} \right)^{p_{ij}} - \left(\frac{\sigma_{ij}}{r_{ij}} \right)^{q_{ij}} \right] \exp \left(\frac{\sigma_{ij}}{r_{ij} - a_{ij} \sigma_{ij}} \right)$$

$$\phi_3(r_{ij}, r_{ik}, \theta_{ijk}) = \lambda_{ijk} \epsilon_{ijk} [\cos \theta_{ijk} - \cos \theta_{0ijk}]^2 \exp \left(\frac{\gamma_{ij} \sigma_{ij}}{r_{ij} - a_{ij} \sigma_{ij}} \right) \exp \left(\frac{\gamma_{ik} \sigma_{ik}}{r_{ik} - a_{ik} \sigma_{ik}} \right)$$

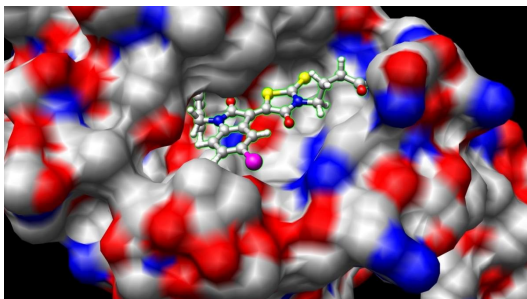
F. H. Stillinger, T. A. Weber; Computer Simulation of Local Order in Condensed Phases of Silicon. *Phys. Rev. B*, **1985**, *31*, 5262–5271.

- 1st Generation Reactive Empirical Bond Order (REBO)
- 2nd Generation REBO
- Adaptive Intermolecular REBO (AIREBO)
- Embedded Ion Method (EIM)
- Environment-Dependent Interatomic Potential (EDIP)
- Angular-Dependent Potential (ADP)
- Bond-Order Potentials (BOP)
- 3-Body Free-Form Potential (Polymorphic)
- Vashishta Family of Potentials
- Charge-Optimized Many-Body Potential (COMB)
- ReaxFF

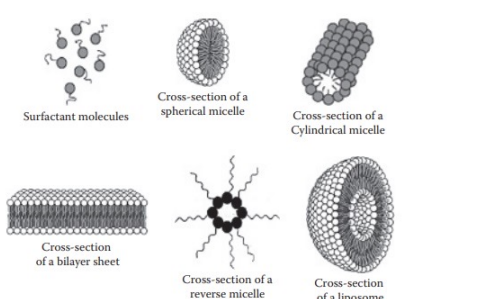
Class I Forcefields

OPLS / CHARMM / AMBER / TraPPE / GROMOS

Computer-Aided Drug Design

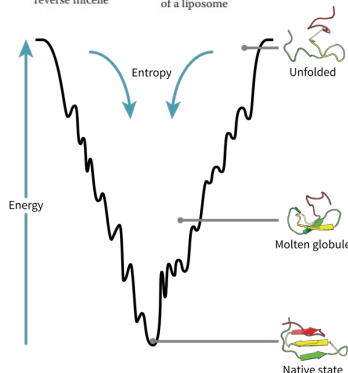
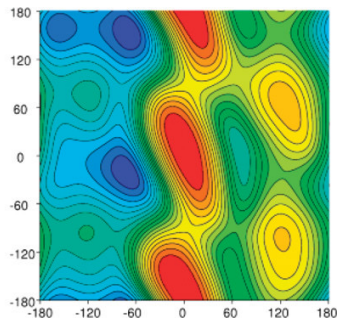
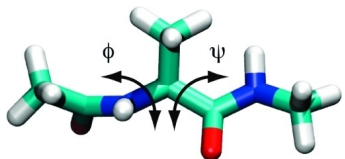


Consumer Products /
Aqueous Simulations



Generalized Sum of
Sinusoidal Torsion Terms

$$E = \sum_{i=1,m} K_i [1.0 + \cos(n_i \phi) - d_i]$$



© Materials Design, Inc. 2023

OPLS-AA

$$E(\phi) = E_{\text{bond}}(\phi) + E_{\text{angle}}(\phi) + E_{\text{n.b.}}(\phi) + E_{\text{torsion}}(\phi)$$

$$E_{\text{ab}} = \sum_i \sum_j^{\text{on a on b}} [q_i q_j e^2 / r_{ij} + 4\epsilon_{ij} (\sigma_{ij}^{12} / r_{ij}^{12} - \sigma_{ij}^6 / r_{ij}^6)] f_{ij}$$

$$E_{\text{bond}} = \sum_{\text{bonds}} K_r (r - r_{\text{eq}})^2$$

$$\sigma_{ij} = \sqrt{\sigma_{ii} \sigma_{jj}}$$

$$E_{\text{angle}} = \sum_{\text{angles}} K_{\theta} (\theta - \theta_{\text{eq}})^2$$

$$\epsilon_{ij} = \sqrt{\epsilon_{ii} \epsilon_{jj}}$$

$$E_{\text{torsion}} = \sum_i \frac{V_1^i}{2} [1 + \cos(\phi_i + f_i1)] + \frac{V_2^i}{2} [1 - \cos(2\phi_i + f_i2)] +$$

$$\frac{V_3^i}{2} [1 + \cos(3\phi_i + f_i3)]$$

W. L. Jorgensen, D. S. Maxwell, J. Tirado-Rives; Development and Testing of the OPLS All-Atom Force Field on Conformational Energetics and Properties of Organic Liquids. *J. Am. Chem. Soc.*, **1996**, *118*, 11225–11236.

In the 1980s and 1990s, large amounts of effort went into empirically parameterizing forcefields that cover a large chemical space for condensed phase systems.

Class II Forcefields

COMPASS / PCFF+

- Accounts for anharmonic and intramolecular coupling interactions.
- Conventionally uses 9-6 LJ form instead of the 12-6 form.
- Sixth-power mixing rules:

$$r^* = [(r_i^{*6} + r_j^{*6})/2]^{1/6}$$

$$\varepsilon = (\varepsilon_i \varepsilon_j)^{1/2} 2(r_i^* r_j^*)^3 / [r_i^{*6} + r_j^{*6}]$$

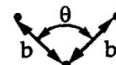
- Attempting to use existing 12-6 LJ parameters in the 9-6 LJ form is not recommended.

$$\begin{aligned}
 E = & \sum_b [{}^2K_b(b - b_0)^2 + {}^3K_b(b - b_0)^3 \\
 & + {}^4K_b(b - b_0)^4] + \sum_\theta [{}^2K_\theta(\theta - \theta_0)^2 \\
 & + {}^3K_\theta(\theta - \theta_0)^3 + {}^4K_\theta(\theta - \theta_0)^4] \\
 & + \sum_\phi [{}^1K_\phi(1 - \cos \phi) + {}^2K_\phi(1 \\
 & - \cos 2\phi) + {}^3K_\phi(1 - \cos 3\phi)] \\
 & + \sum_{i>j} \frac{q_i q_j}{r_{ij}} + \sum_{i>j} \varepsilon \left[2 \left(\frac{r^*}{r_{ij}} \right)^9 - 3 \left(\frac{r^*}{r_{ij}} \right)^6 \right] \\
 & + \sum_b \sum_{b'} K_{bb'}(b - b_0)(b' - b'_0) \\
 & + \sum_\theta \sum_{\theta'} K_{\theta\theta'}(\theta - \theta_0)(\theta' - \theta'_0) \\
 & + \sum_b \sum_\theta K_{b\theta}(b - b_0)(\theta - \theta_0) \\
 & + \sum_\phi \sum_b (b - b_0)[{}^1K_{\phi b} \cos \phi \\
 & + {}^2K_{\phi b} \cos 2\phi + {}^3K_{\phi b} \cos 3\phi] \\
 & + \sum_\phi \sum_{b'} (b' - b'_0)[{}^1K_{\phi b'} \cos \phi \\
 & + {}^2K_{\phi b'} \cos 2\phi + {}^3K_{\phi b'} \cos 3\phi] \\
 & + \sum_\phi \sum_\theta (\theta - \theta_0)[{}^1K_{\phi\theta} \cos \phi \\
 & + {}^2K_{\phi\theta} \cos 2\phi + {}^3K_{\phi\theta} \cos 3\phi] \\
 & + \sum_\phi \sum_\theta \sum_{\theta'} K_{\phi\theta\theta'}(\theta - \theta_0)(\theta' - \theta'_0) \cos \phi
 \end{aligned}$$

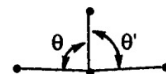
a. bond/bond



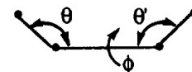
b. bond/angle



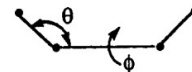
c. angle/angle



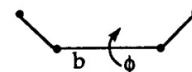
d. angle/angle/torsion



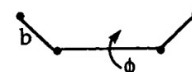
e. angle/torsion



f. bond/torsion (type 1)

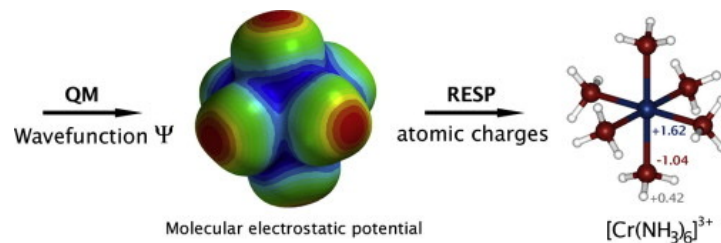


g. bond/torsion (type 2)



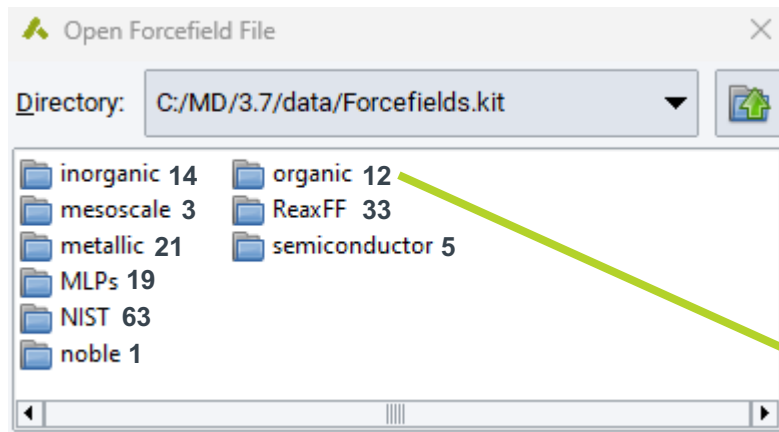
Challenges of Atom Typing

- Defined by intramolecular structure
 - Repulsion–dispersion interactions rely upon standard mixing rules or explicit IJ parameterization.
 - Partial charges are static, but the electrostatic potential is dependent on the local chemical environment.
 - Charge equilibration or polarization methods attempt to address this but add another layer of parameters and significantly increase computational expense.
- Complexity of specification
 - Alternative parameter assignment formalisms have been developed to limit complexity of parameter specification.
 - D.L. Mobley et al., Escaping Atom Types in Force Fields Using Direct Chemical Perception. **2018**, *14*, 6076–6092.

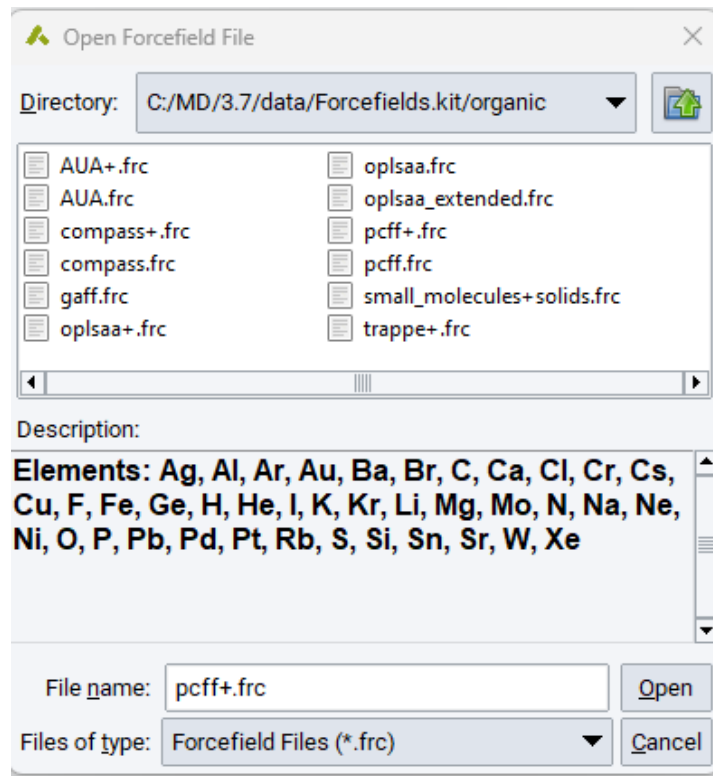
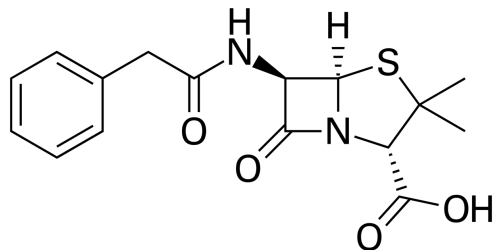


I. Djordjević, S.R. Niketić, *Comp. Theor. Chem.*, **2012**, *1001*, 20–25.

Assigning FF Parameters is Easy ... With *MedeA*!



Penicillin G

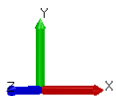
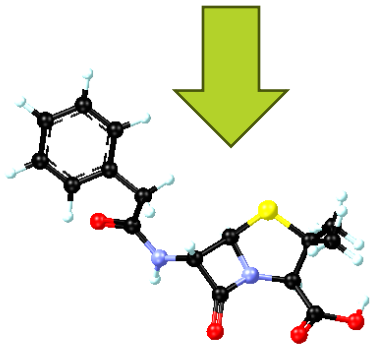


MedeA: provide a SMILES

Create a new molecule provided its SMILES string (Simplified Molecular Input Line Entry Specification)

Title:

SMILES:



Atom	Name	Element	Atomic Number	Wyckoff Position	Wyckoff Equation	X	Y	Z	Freeze	Occupancy	Spin	FF Atom Type	FF Charge
1	O1	O	8	1a	x,y,z	0.223259	0.525295	0.490271	---	1	0	o_1	-0.45
		C	6	1a	x,y,z	0.316005	0.514904	0.499452	---	1	0	c_1	0.45
		C	6	1a	x,y,z	0.373673	0.593356	0.567263	---	1	0	c2	-0.106
		C	6	1a	x,y,z	0.309836	0.664443	0.628657	---	1	0	cp	0
		C	6	1a	x,y,z	0.232433	0.623576	0.679464	---	1	0	cp	-0.1268
		C	6	1a	x,y,z	0.169662	0.688141	0.731644	---	1	0	cp	-0.1268
		C	6	1a	x,y,z	0.185376	0.794674	0.734357	---	1	0	cp	-0.1268
		C	6	1a	x,y,z	0.26494	0.835666	0.685103	---	1	0	cp	-0.1268
		C	6	1a	x,y,z	0.327496	0.770107	0.632634	---	1	0	cp	-0.1268
10	N1	N	7	1a	x,y,z	0.365496	0.428472	0.44486	---	1	0	n_31	-0.46
11	O9	O	8	1a	x,y,z	0.466	0.427882	0.462566	---	1	0	c4h1	0.057
12	C10	C	6	1a	x,y,z	0.52065	0.332944	0.431602	---	1	0	c_1	0.45
13	O2	O	8	1a	x,y,z	0.526012	0.235751	0.475983	---	1	0	o_1	-0.45
14	N2	N	7	1a	x,y,z	0.564281	0.382925	0.344918	---	1	0	n_30	-0.42
15	C11	C	6	1a	x,y,z	0.514559	0.48453	0.353457	---	1	0	c4h1	0.132
16	S	S	16	1a	x,y,z	0.615575	0.555835	0.355292	---	1	0	sc	-0.25
17	C12	C	6	1a	x,y,z	0.69362	0.47404	0.276577	---	1	0	c0	0.125
18	C13	C	6	1a	x,y,z	0.645179	0.367588	0.27298	---	1	0	c5h1	0.007
19	C14	C	6	1a	x,y,z	0.715168	0.281766	0.296786	---	1	0	c_1	0.562
20	O3	O	8	1a	x,y,z	0.714384	0.227375	0.395707	---	1	0	o_1	-0.45
21	O4	O	8	1a	x,y,z	0.786199	0.260203	0.208161	---	1	0	o_2c	-0.535
22	C15	C	6	1a	x,y,z	0.704141	0.51145	0.156626	---	1	0	c3	-0.159
23	C16	C	6	1a	x,y,z	0.782551	0.475485	0.348298	---	1	0	c3	-0.159
24	H1	H	1	1a	x,y,z	0.417232	0.637783	0.50978	---	1	0	hc	0.053
25	H2	H	1	1a	x,y,z	0.416613	0.552278	0.628259	---	1	0	hc	0.053
26	H3	H	1	1a	x,y,z	0.22106	0.540283	0.678284	---	1	0	hc	0.1268
27	H4	H	1	1a	x,y,z	0.108298	0.655878	0.770401	---	1	0	hc	0.1268
28	H5	H	1	1a	x,y,z	0.135683	0.845583	0.774175	---	1	0	hc	0.1268
29	H6	H	1	1a	x,y,z	0.27786	0.918446	0.687933	---	1	0	hc	0.1268
30	H7	H	1	1a	x,y,z	0.39011	0.801266	0.594747	---	1	0	hc	0.1268
31	H8	H	1	1a	x,y,z	0.331291	0.372701	0.393109	---	1	0	hn2	0.35
32	H9	H	1	1a	x,y,z	0.487048	0.461843	0.542589	---	1	0	hc	0.053
33	H10	H	1	1a	x,y,z	0.470532	0.496725	0.280396	---	1	0	hc	0.053
34	H11	H	1	1a	x,y,z	0.620539	0.355806	0.187589	---	1	0	hc	0.053
35	H12	H	1	1a	x,y,z	0.779183	0.315285	0.142054	---	1	0	ho2	0.423
36	H13	H	1	1a	x,y,z	0.637208	0.505224	0.114364	---	1	0	hc	0.053
37	H14	H	1	1a	x,y,z	0.753551	0.463065	0.112862	---	1	0	hc	0.053
38	H15	H	1	1a	x,y,z	0.726823	0.590729	0.156078	---	1	0	hc	0.053
39	H16	H	1	1a	x,y,z	0.767778	0.450021	0.434401	---	1	0	hc	0.053
40	H17	H	1	1a	x,y,z	0.809247	0.554543	0.350659	---	1	0	hc	0.053
41	H18	H	1	1a	x,y,z	0.833632	0.425207	0.310165	---	1	0	hc	0.053

Periodic structure 41 atoms 43 bonds

MedeA Automatically Generates LAMMPS-Style Input Files

Data File

```
LAMMPS Description

  41 atoms
  43 bonds
  77 angles
  83 dihedrals
  39 impropers

  15 atom types
  24 bond types
  47 angle types
  40 dihedral types
  27 improper types

# Cell: 14.563000 12.947900 11.810400 90.0000 90.0000 90.0000
  0.000000 14.563000 xlo xhi
  0.000000 12.947900 ylo yhi
  0.000000 11.810400 zlo zhi

Masses

   1 12.01115 # c0
   2 12.01115 # c2
   3 12.01115 # c3
   4 12.01115 # c4h1
   5 12.01115 # c5h1
   6 12.01115 # c_1
   7 12.01115 # cp
   8 1.00797 # hc
   9 1.00800 # hn2
  10 1.00800 # ho2
  11 14.00670 # n_30
  12 14.00670 # n_31
  13 15.99940 # o_1
  14 15.99940 # o_2c
  15 32.06400 # sc

Atoms

 1 1 13 -0.45000000 3.251325 6.801469 5.790298 0 0 0 # O1 o_1
 2 1 6 -0.45000000 4.601975 6.666929 5.898726 0 0 0 # C1 c_1
 3 1 2 -0.10600000 5.441805 7.682719 6.699609 0 0 0 # C2 c_2
 4 1 7 0.00000000 4.512145 8.603138 7.424688 0 0 0 # C3 cp
 5 1 7 -0.12680000 3.384923 8.073994 8.024746 0 0 0 # C4 cp
 6 1 7 -0.12680000 2.470782 8.909986 8.641007 0 0 0 # C5 cp
 7 1 7 -0.12680000 2.699637 10.289356 8.673048 0 0 0 # C6 cp
 8 1 7 -0.12680000 3.858314 10.820120 8.091341 0 0 0 # C7 cp
 9 1 7 -0.12680000 4.769317 9.971263 7.471657 0 0 0 # C8 cp
10 1 12 -0.46000000 5.322718 5.547815 5.253976 0 0 0 # N1 n_31
11 1 4 0.05700000 6.786354 5.540178 5.463092 0 0 0 # C9 c4h1
12 1 6 0.45000000 7.582232 4.310931 5.097394 0 0 0 # C10 c_1
13 1 13 -0.45000000 7.660312 3.052479 5.621550 0 0 0 # O2 o_1
14 1 11 -0.12000000 8.217620 4.958074 4.073620 0 0 0 # N2 n_30
15 1 4 0.13200000 7.493518 6.273652 4.174465 0 0 0 # C11 c4h1
```

Parameter File

```
bond_coeff 1 1.202 851.14 -1918.5 2160.8 # c_1 o_1
bond_coeff 2 1.4902 253.71 -423.04 396.9 # c_1 c_1
bond_coeff 3 1.501 321.9 -521.82 572.16 # c cp
bond_coeff 4 1.417 470.84 -627.62 1327.6 # cp cp
bond_coeff 5 1.336 390.68 -768.38 923.24 # c_1 n_2
bond_coeff 6 1.4432 319.16 -586.32 961.41 # c n_2
bond_coeff 7 1.4902 253.71 -423.04 396.9 # c_1 c_1
bond_coeff 8 1.356 390.68 -768.38 923.24 # c_1 n_30
bond_coeff 9 1.4532 319.16 -586.32 961.41 # c n_30
bond_coeff 10 1.53 299.67 -501.77 679.81 # c c
bond_coeff 11 1.823 225.28 -327.71 488.97 # c s
bond_coeff 12 1.823 225.28 -327.71 488.97 # c s
bond_coeff 13 1.53 299.67 -501.77 679.81 # c c
bond_coeff 14 1.4532 319.16 -586.32 961.41 # c n_30
bond_coeff 15 1.4902 253.71 -423.04 396.9 # c_1 c_1
bond_coeff 16 1.3683 367.15 -794.79 1055.2 # c_1 o_2
bond_coeff 17 1.53 299.67 -501.77 679.81 # c c
bond_coeff 18 1.101 345 -691.89 844.6 # c h
bond_coeff 19 1.0982 372.83 -803.45 894.32 # cp h
bond_coeff 20 0.9959 495.83 -1092.7 1441.1 # hn2 n_2
bond_coeff 21 1.101 345 -691.89 844.6 # c h
bond_coeff 22 1.101 345 -691.89 844.6 # c h
bond_coeff 23 0.952 534.3 -1287.2 1889.1 # ho2 o_2
bond_coeff 24 1.101 345 -691.89 844.6 # c h
angle_coeff 1 123.15 55.543 -17.212 0.1348 # c c_1 o_1
angle_coeff 2 125.53 101.88 -41.809 0 # n_2 c_1 o_1
angle_coeff 3 116.93 39.419 -10.995 -8.7733 # c c_1 n_2
angle_coeff 4 109.5 60 0 0 # * c_1 *
angle_coeff 5 107.73 40.61 -28.812 0 # c_1 c h
angle_coeff 6 111 44.323 -9.4454 0 # cp c h
angle_coeff 7 107.66 39.641 -12.921 -2.4318 # h c h
angle_coeff 8 120.05 44.715 -22.735 0 # c cp cp
angle_coeff 9 118 0 61 0 33 34 0 0 0 # cp cp cp
```

Input File

```
# This is the control script for LAMMPS.

echo both
log 1.1_Initialize.out

#-----
# Stage 1.1: Initialize LAMMPS run for 3-d periodic
#-----

units real
boundary p p p
atom_style full

pair_style lj/class2/coul/long 9.5
pair_modify mix sixthpower
pair_modify tail yes
bond_style class2
angle_style class2
dihedral_style class2
improper_style class2
special_bonds lj 0.0 0.0 1.0 coul 0.0 0.0 1.0

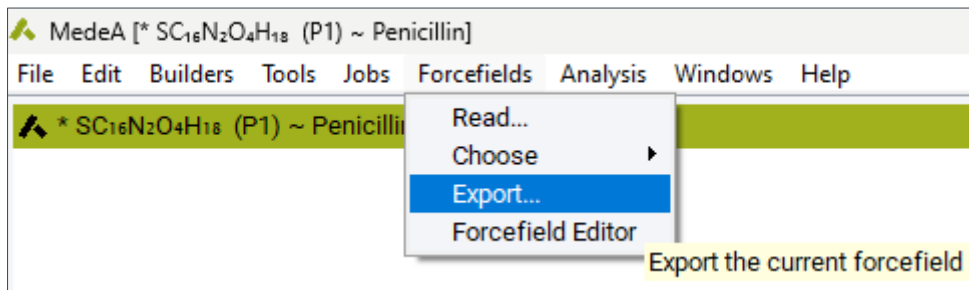
box tilt large
read_data structure.dat

include parameters.dat

neighbor 2.0 bin
neigh_modify delay 0 every 1 check yes
kspace_style pppm 0.0001
```

All files are in plaintext and readable. Full transparency.

Customizing MedeA FRC Files



The FRC file format is well documented!

FRC Forcefield Files in MedeA

Contents

- *Introduction*
- *Getting Started*
- *Forcefield Type*
- *Versions and References*
- *Description*
- *Inclusion of Other FRC File(s)*
- *Definition of Forcefield*
- *Forcefields with MedeA-LAMMPS and MedeA-GIBBS*

Examples of Oxygen Atom Typing via Templates

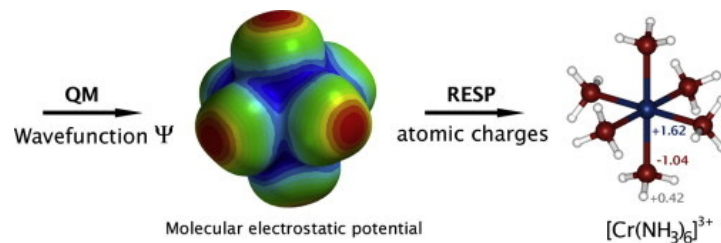
```
type oh
! oxygen bonded to hydrogen
template (>O(-H)(-*))
end_type
```

```
type: oc
! SP3 oxygen in ether or acetals
template (>O(-C)(-C))
atom_test:1
aromaticity:NON_AROMATIC
end_test
end_type
```

```
type: oe
! SP3 oxygen in ester
template (>O(-C(=O))(-C))
atom_test:1
aromaticity:NON_AROMATIC
end_test
end_type
```

Challenges of Atom Typing

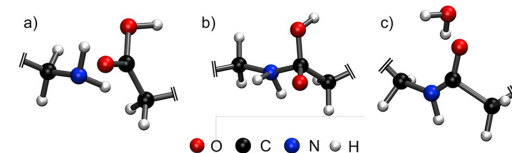
- Defined by intramolecular structure
 - Repulsion–dispersion interactions rely upon standard mixing rules or explicit IJ parameterization.
 - Partial charges are static, but the electrostatic potential is dependent on the local chemical environment.
 - Charge equilibration or polarization methods attempt to address this but add another layer of parameters and significantly increase computational expense.
- Complexity of specification
 - Alternative parameter assignment formalisms have been developed to limit complexity of parameter specification.
 - D.L. Mobley et al., Escaping Atom Types in Force Fields Using Direct Chemical Perception. **2018**, *14*, 6076–6092.



I. Djordjević, S.R. Niketić, *Comp. Theor. Chem.*, **2012**, *1001*, 20–25.

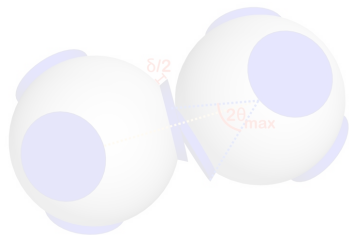
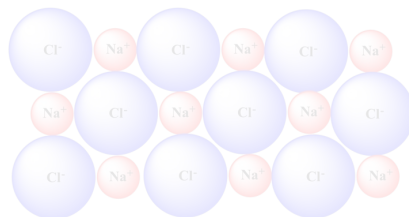
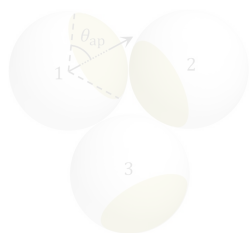
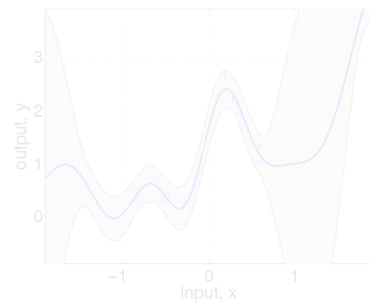
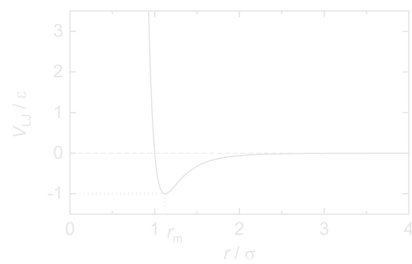
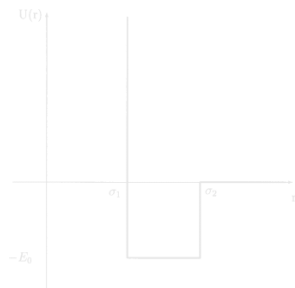
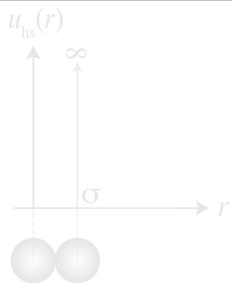
- Reactions require atom type changes
 - Reactions can be facilitated by mapping atom types and bonding topology between reactant and product templates.
 - J.R. Gissinger, B.D. Jensen, K.E. Wise; Modeling Chemical Reactions in Classical Molecular Dynamics Simulations. *Polymer*, **2017**, *128*, 211–217.
 - J.R. Gissinger, B.D. Jensen, K.E. Wise; REACTER: A Heuristic Method for Reactive Molecular Dynamics. *Macromolecules*, **2020**, *53*, 9953–9961.

Polycondensation of Nylon 6,6 using *fix bond/react*



Versatility of Functional Form

Embellishments and Complexity



Machine-Learned Potentials

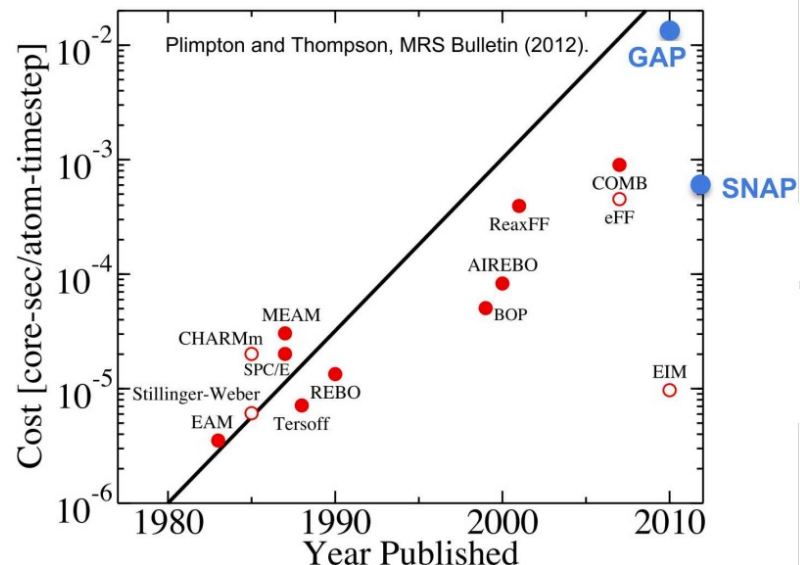
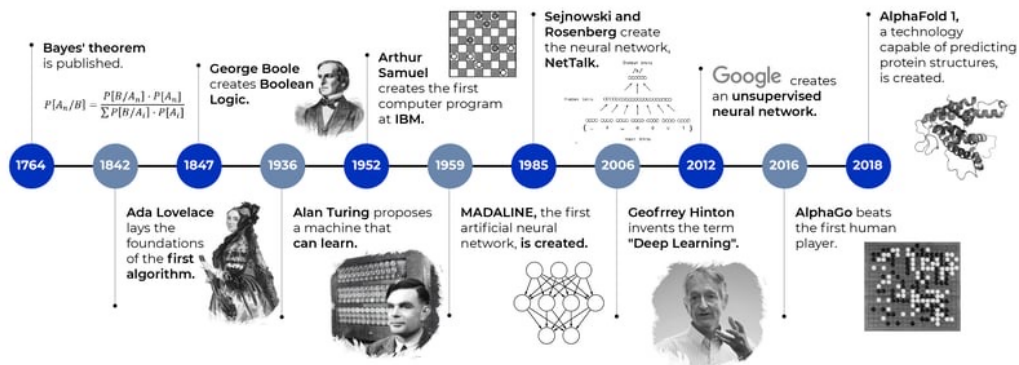
A rose by any other name ...

- Machine learning potential (MLP)
- Machine learning interatomic potential (MLIP / ML-IAP)
- Machine learning forcefield (MLFF)

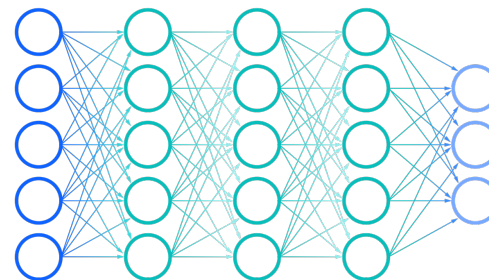
Potentials available in LAMMPS

- Gaussian Approximation Potential (GAP)
- Spectral Neighbor Analysis Potential (SNAP)
- High-Dimensional Neural Network Potential (HDNNP)

MACHINE LEARNING TIMELINE

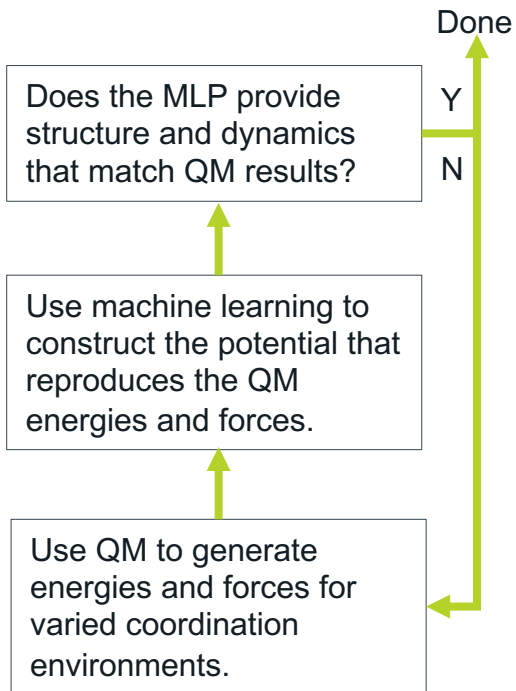


<https://www.osti.gov/servlets/purl/1639258>

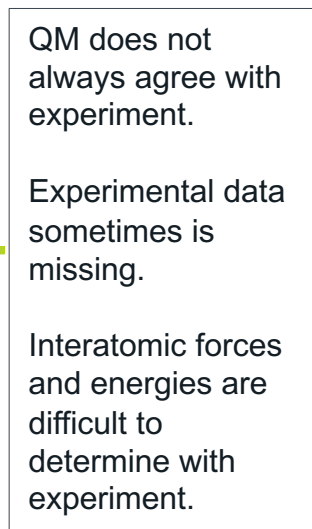


Training Machine-Learned Potentials

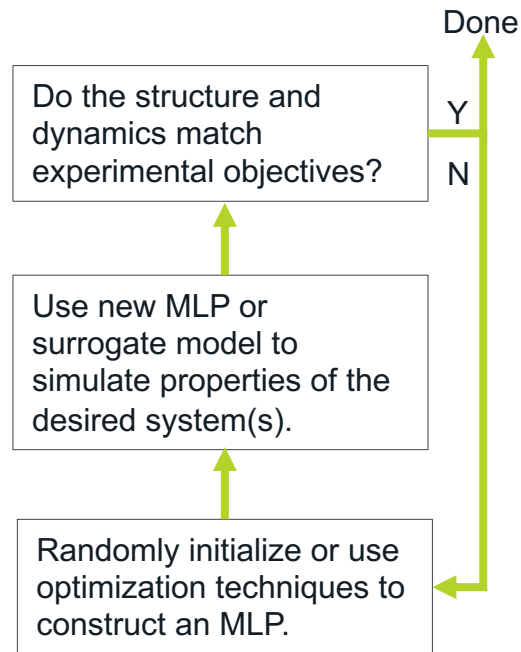
First-Principles



Hybrid



Empiricism



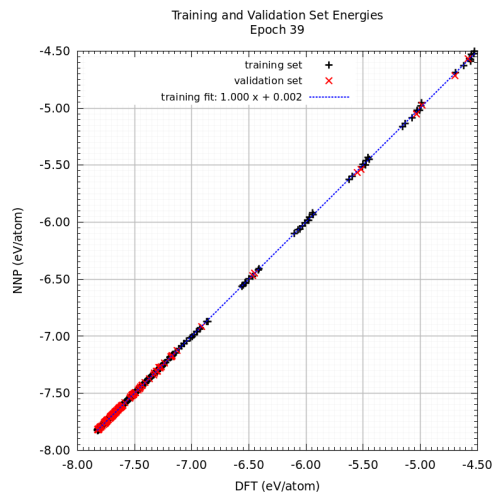
Generating Training Data for MLPs using *MedeA VASP*

1. Use “sloppy” trajectories to quickly generate both low-energy and high-energy configurations.
2. Run higher quality single-point energy (SPE) calculations for configurations that are not too correlated.
3. Combine all SPE results into a Fitting Training Sets (FTS) file.

The screenshot shows the MedeA: Run VASP 6 interface. The 'Type of calculation' is set to 'Molecular Dynamics'. Under 'Molecular Dynamics Parameters', the 'Ensemble' is 'isothermal-isobaric (NPT)'. Simulation time is 1000 fs, and the time step is 4.0 fs. The trajectory file frequency is 1 steps. Temperature initial is 298.0 K. The 'Task' is 'Create forcefield by on-the-fly learning'. The 'Interaction' section shows 'Density functional' and 'GGA-PBE'. The 'General Setup' section shows 'Precision' set to 'Low' and 'Plane-wave cutoff' set to 200 eV.

The screenshot shows the MedeA: Run VASP 6 interface. The 'Type of calculation' is set to 'Single Point'. Under 'Single Point Parameters', the 'Apply machine-learned forcefield' checkbox is checked. The 'Interaction' section shows 'Density functional' and 'GGA-PBE'. The 'General Setup' section shows 'Precision' set to 'Accurate' and 'Plane-wave cutoff' set to 520 eV.

Training MLPs is Easy With *MedeA MLPG!*



Main >>

Start

MLP Generator

Potential: SNAP
Band limit: 8
Radial cutoff: 4.8
Fitting: energy forces stress

Edit stage: MLP Generator

Training set: C:/Users/GarrettTow/training_data.fts Select ...

Δ -learning:
 Δ -learning potential: Select ...

Type of machine-learned potential: SNAP

Parameters for SNAP Advanced Spin parameters

Band limit: 8

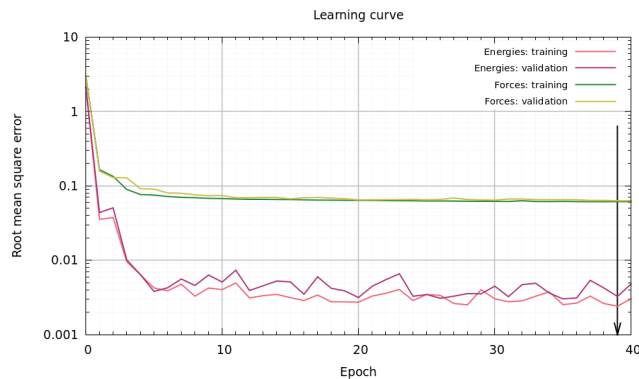
Radial cutoff: 4.8

Fraction of data to use as test set: 0.1

Element	Relative radius	Weight	Energy shift
	0.5	1.0	0.0

Fit:
Weights:

<input checked="" type="checkbox"/> Energy	<input checked="" type="checkbox"/> Forces	<input checked="" type="checkbox"/> Stress
1.0	0.01	1.0e-06



Potentials Currently Available for Training:

- Spectral Neighbor Analysis Potential (SNAP)
- High-Dimensional Neural Network Potential (HDNNP)
- Atomic Cluster Expansion (ACE)

Pros and Cons of Machine-Learned Potentials

Pros

- Elemental description; no atom types
- Short-ranged potentials; typically no charges
- No fixed bonds; reactivity allowed
- A potential can model multiple oxidation states
- Near-DFT accuracy but can simulate 10,000+ atom systems

Unclear how much training data is initially needed.
Iterative process that requires adding “missing structures” as needed.

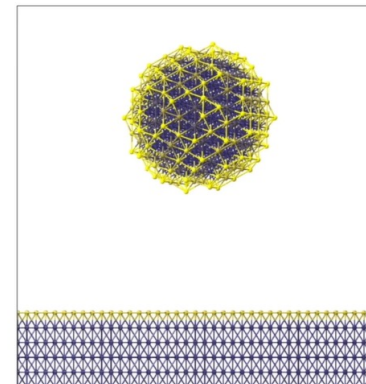
Cons

- Difficult, if not impossible, to physically interpret
- Poor extrapolation beyond training conditions
- Lack of transferability and “mixing rules”



Machine-Learned Potentials:
Surpassing the Limits of the
ab initio World without
leaving it behind

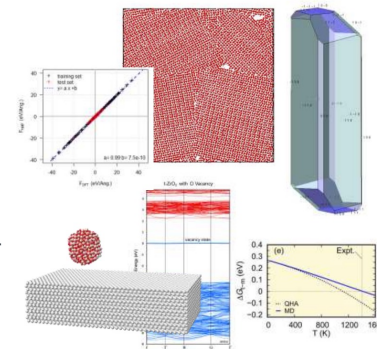
August 1-3, 2023



VASP, Machine Learning, and
Multi-Scale Physics: Defining the
State of the Art in Materials
Modeling

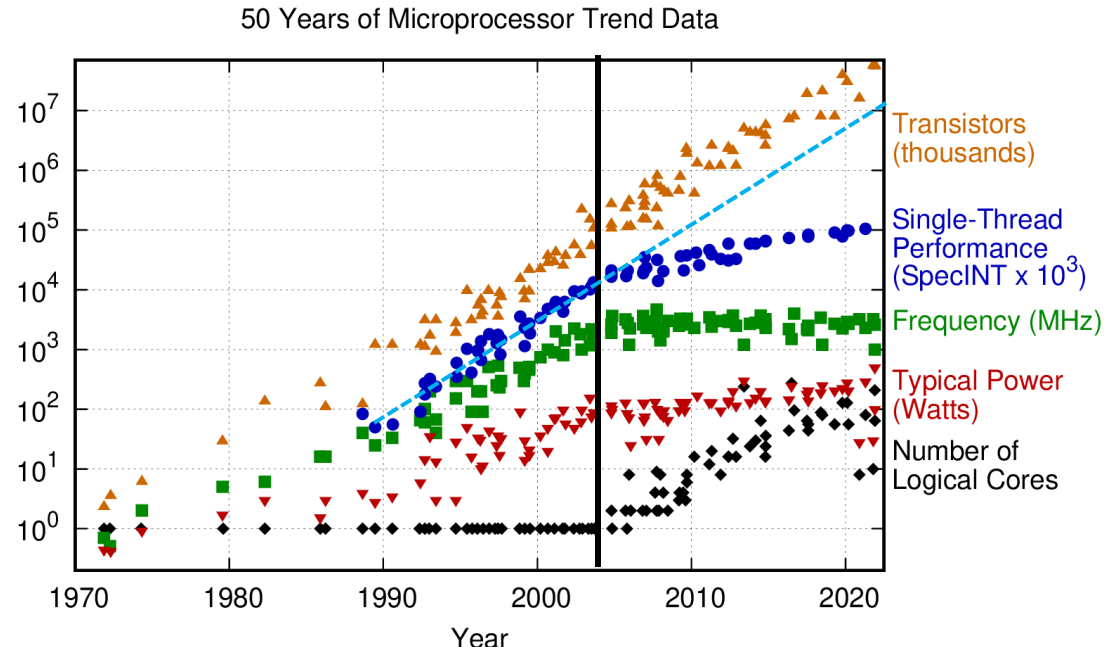
Martijn Marsman, University of Vienna and VASP GmbH
Erich Wimmer, Materials Design, Inc.

16-18 August 2022



Microprocessor Trends Influence Forcefield Development

- 2004 marks the transition from frequency scaling to parallel computing.
- Single-thread performance keeps slightly improving through:
 - Techniques granting more instructions per clock cycle.
 - Clever power management
 - Dynamic clock frequency
- Currently, processors are being shipped with 128/256 physical/logical cores.



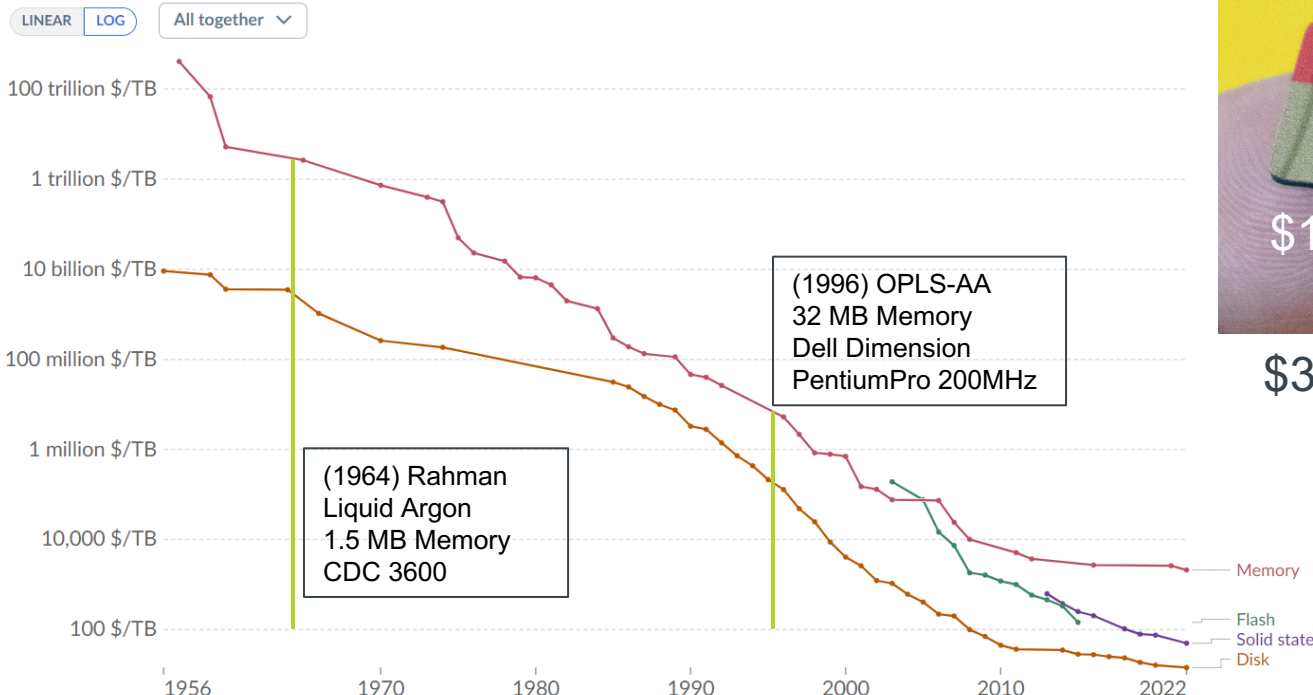
Original data up to the year 2010 collected and plotted by M. Horowitz, F. Labonte, O. Shacham, K. Olukotun, L. Hammond, and C. Batten
New plot and data collected for 2010-2021 by K. Rupp

<https://github.com/karlrupp/microprocessor-trend-data>

Computing Costs – Memory and Storage

Historical cost of computer memory and storage

This data is expressed in US dollars per terabyte (TB). It is not adjusted for inflation.



Source: John C. McCallum (2022)

Note: For each year, the time series shows the cheapest historical price recorded until that year.

OurWorldInData.org/technological-change • CC BY

© Materials Design, Inc. 2023



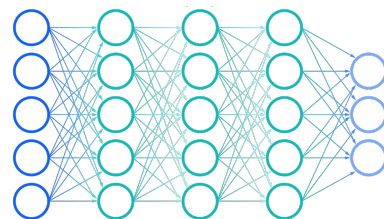
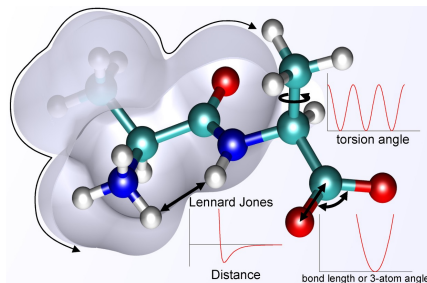
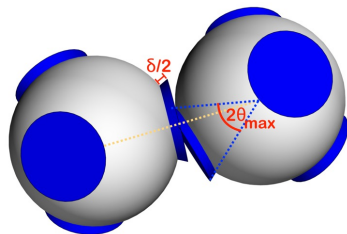
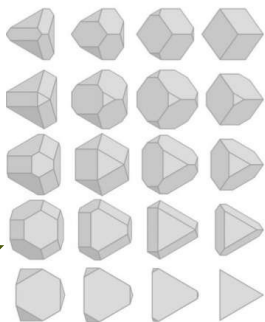
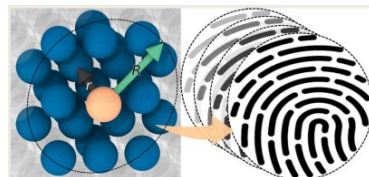
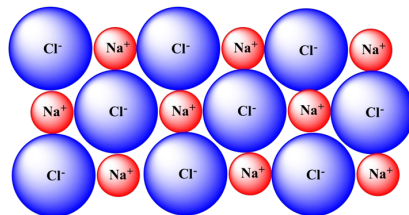
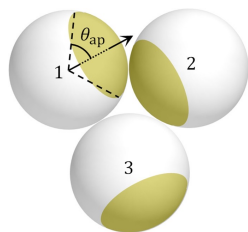
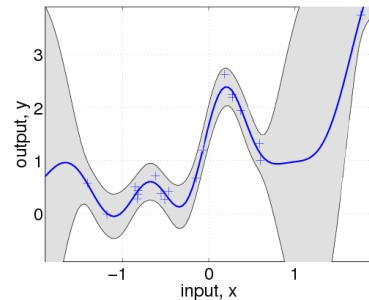
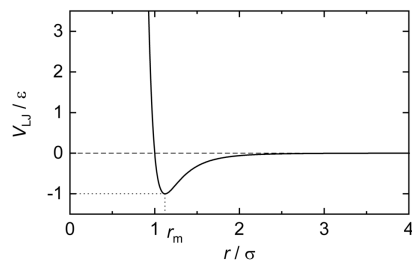
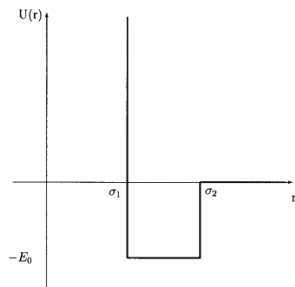
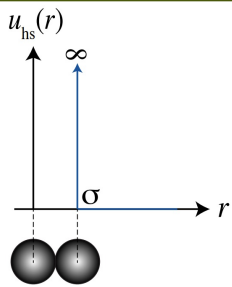
Mercury delay-line memory of UNIVAC
1000 words – 12 characters per word
(1951)



IBM 350 Disk Drive
3.75 MB (1956)

Versatility of Functional Form

Embellishments and Complexity



Relevant *MedeA* Modules

MedeA Environment: Materials Modelling and Simulation Environment

MedeA EAM: A forcefield based simulations provide computationally efficient descriptions of the structural, mechanical, and dynamical properties of metallic systems.

MedeA ReaxFF: A well-established formalism of variable charge, reactive forcefield widely used in forcefield based simulations by the computational materials scientists in both academic and industrial communities.

MedeA Forcefield Optimizer (FFO): Determines optimum forcefield parameters for energy minimization (EM), molecular dynamics (MD), and Monte Carlo (MC) simulations.

MedeA MLP: Machine Learning Potential (MLP) based simulations using *MedeA LAMMPS* carry the accuracy known from first principles calculations to length and time scales, which are orders of magnitude larger, at much lower computational cost. A number of example MLPs from the literature are provided with *MedeA MLP*. In addition, MLPs created by the *MedeA MLP Generator (MLPG)* can be used.

MedeA MLPG: The Machine Learning Potential Generator (MLPG) forms the centerpiece of Machine Learning materials research by transferring the high accuracy of first principles calculations to the realm of very efficient forcefield simulations. The MLPG builds on training sets consisting of energies, forces, and stresses calculated from first principles for a variety of systems and uses machine learning techniques to create from these training sets parametrized descriptions of the energy/forces/stresses hypersurface. Machine learning potentials generated by the MLPG are ready for immediate use with *MedeA MLP*.

MedeA VASP: The Vienna Ab initio Simulation Package (VASP) is the leading electronic structure program for solids, surfaces, and interfaces. VASP is an extremely well tested, robust, and proven program for calculations based on local and semi-local density functional theory (DFT) applying plane wave basis sets. In addition, VASP provides advanced methods beyond DFT to calculate electronic structure and response, as well as energies of very high accuracy.

Related *MedeA* Webinars

Machine-Learned Potentials: Surpassing the Limits of the ab initio World without leaving it behind:

<https://www.materialsdesign.com/webinars/recorded/mlp-surpassing-the-limits-of-ab-initio>

On-the-fly Machine Learning Forcefields with MedeA VASP:

<https://www.materialsdesign.com/webinars/recorded/MedeA-Training-On-the-fly-Machine-Learning-Forcefields-with-MedeA-VASP>

Δ -Machine Learning Beyond DFT: from Phase Transitions to Quantum Paraelectricity and CO Adsorption:

<https://www.materialsdesign.com/webinars/recorded/Delta-Machine-Learning-Beyond-DFT%3A-from-Phase-Transitions-to-Quantum-Paraelectricity-and-CO-Adsorption>

Training: Generating and Applying Machine-Learned Potentials with MedeA:

<https://www.materialsdesign.com/webinars/recorded/UGMtraining-Generating-and-Applying-Machine-Learned-Potentials-with-MedeA>

Atomistic Simulations with High-Dimensional Neural Network Potentials:

<https://www.materialsdesign.com/webinars/recorded/Atomistic-Simulations-with-High-Dimensional-Neural-Network-Potentials>

Atomistic-scale simulations of realistic, complex, reactive materials: the ReaxFF reactive force field and its industrial and academic applications:

<https://www.materialsdesign.com/webinars/recorded/ReaxFF-reactive-force-field>

Materials Design UGM 2023

Vienna, Austria

October 9-11, 2023

<https://www.ugm.materialsdesign.com/>

Professor Georg Kresse (University of Vienna, Austria)

Professor Michele Parrinello (Italian Institute of Technology, Italy; ETH Zurich, Switzerland)

Professor Saad Fahaid Khalaf Al-Afnan (KFUPM, Saudi Arabia)

Anders Engström (CEO, Thermo-Calc, Sweden)

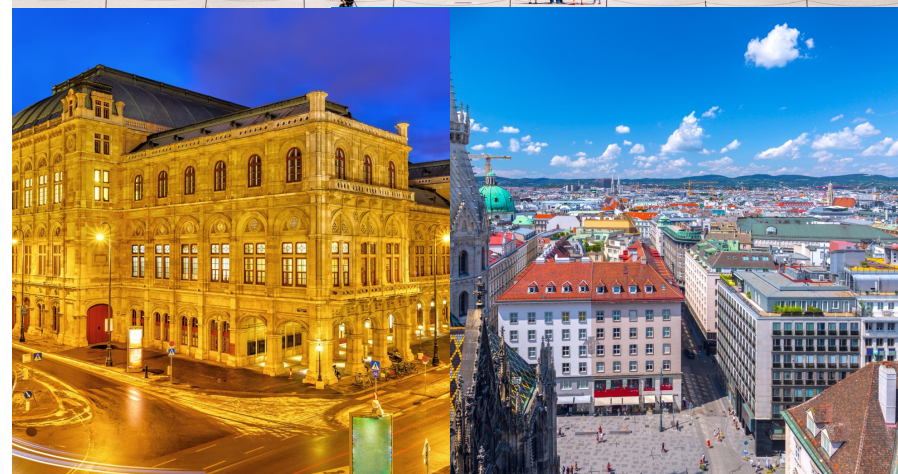
Professor Phuti Ngoepe (University of Limpopo, South Africa)

Professor Ralf Drautz (Ruhr-Universität Bochum, Germany)

Kyle Starkey, Leonid Kahle: (Materials Design, USA)

Edwin Knobbe, René Windiks: (BMW, Germany; Materials Design, USA)

Thomas Pigeon (French Institute of Petroleum Energies - IFPEN, France)



Materials Design UGM 2023

Vienna, Austria

Monday, October 9, 2023

More information

<https://www.ugm.materialsdesign.com/>



Question and Answer Session



Dr. Garrett Tow

Materials Design

Questions about Materials Design Webinars

Katherine Hollingsworth

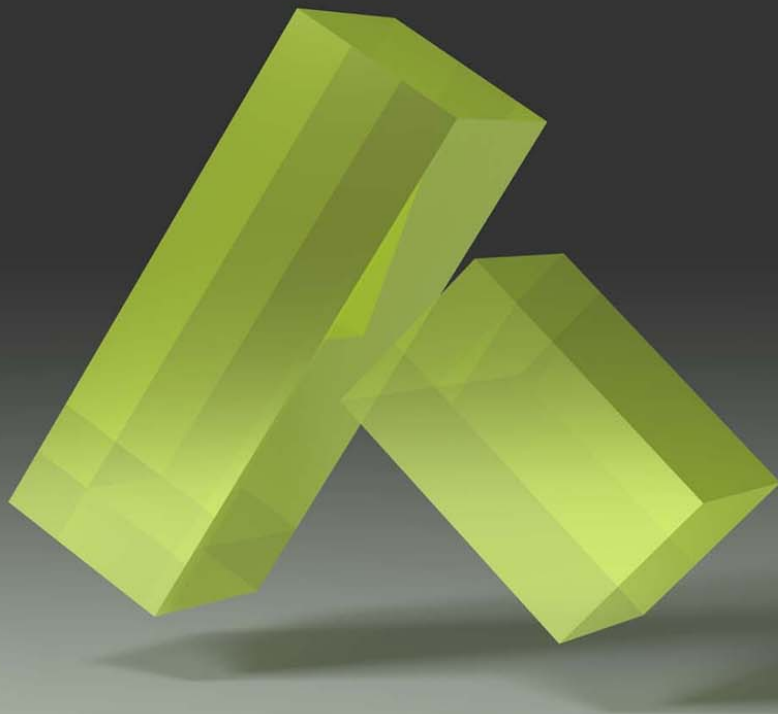
khollingsworth@materialsdesign.com



materials design

info@materialsdesign.com

www.materialsdesign.com



MedeA

Innovation by Simulation

The Price of Power

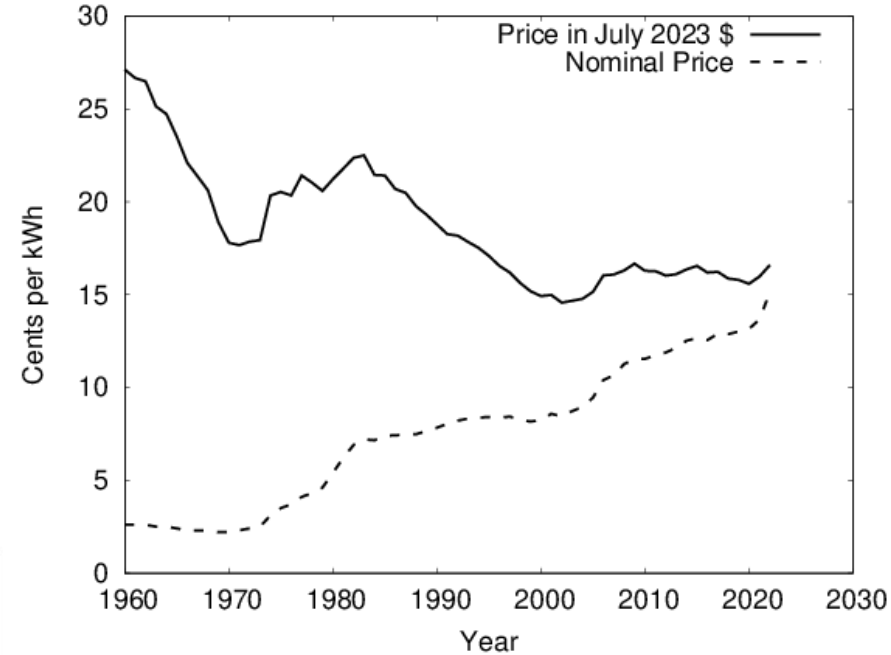
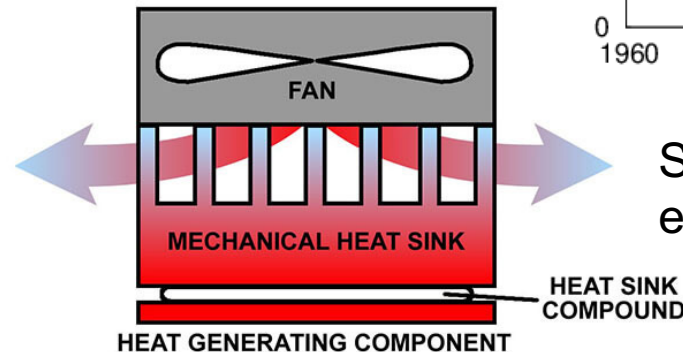
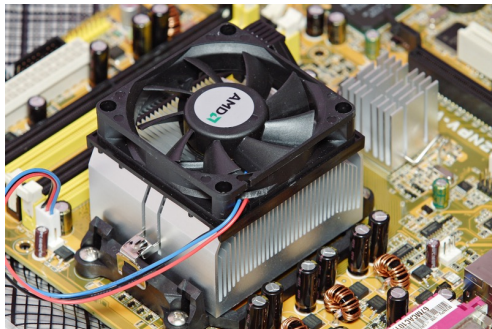
$$P = C * V^2 * F$$

P = Power consumption

C = Capacitance switched per clock cycle

V = Voltage

F = Frequency (cycles per second)

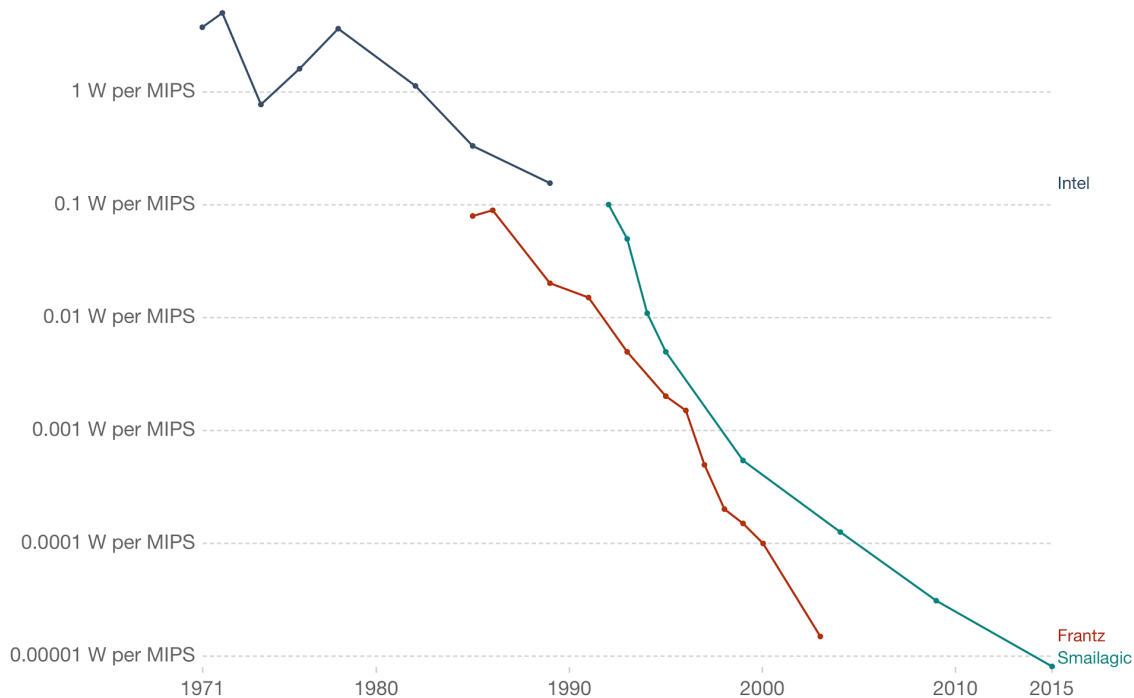


Since 1960, the real price of electricity has dropped by ~40%.

Watts per Million Instructions per Second

Computing efficiency, 1971 to 2015

Computer processing efficiency, measured as the number of watts needed per million instructions per second (Watts per MIPS).



Source: Ray Kurzweil (2005, updated). The Singularity is Near.

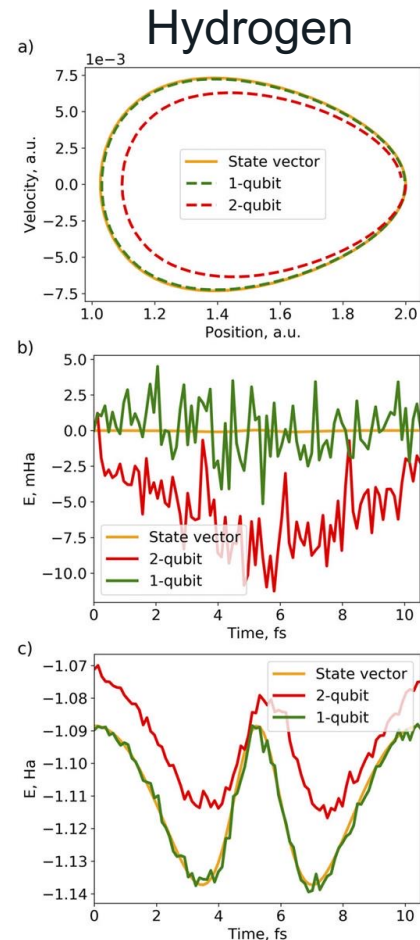
CC BY

What About Quantum Computing?

- More applicable to QM calculations; classical computing better for classical potentials.
- QM calculations could *eventually* be accelerated by quantum computing.
 - Accelerates the development or on-the-fly refinement of machine-learned potentials.

“Today’s quantum computers are generally in the range of 5-100 qubits, whereas solving Shor’s algorithm or **simulating a useful molecule will require thousands to millions of qubits**. Another major issue is fidelity. Due to the sensitive and analog nature of quantum computers, they are inherently **error-prone**, and errors in each logical operation accumulate through the duration of a quantum circuit. The error rates of today’s quantum computers limit them to running only a few logical operations with consistency before **accumulated errors lead to a random result**. This is impractical as applications with known algorithmic speedups require thousands to millions of operations to be run.”

<https://resources.nvidia.com/en-us-hpc-ebooks/hpc-for-the-age-of-ai?xs=409135>



This potential energy shift in the two-qubit system is easily explained by the **hardware noise** from four CNOT gates, which are not present in the one-qubit system; each of the CNOT gates has an error rate on the order of 1%.

D.A. Fedorov et al. *Ab initio* Molecular Dynamics on Quantum Computers. *J. Chem. Phys.* **2021**, *154*, 164103.